

Formaldehyde production from isoprene oxidation across NO_x regimes

Wolfe et al., ACP (2015)

Reviewer Responses

We are grateful to all three reviewers for their insightful comments. A number of changes have been made to the manuscript following these reviews, as detailed below. Referee comments are given in **bold**.

Referee 1

The authors present an investigation of HCHO production over the US based on aircraft measurements, and use the comparisons in smart ways to test current chemical models and their representation of NO_x-dependent reaction pathways of isoprene oxidation. The analysis framework is clear and well-thought out, the writing is clear, and overall the work makes a useful contribution to the literature in this area. The paper should be accepted. Below are just a few comments for the authors to consider.

Abstract (and page 31603), “we find that the total organic peroxy radical production rate is essentially independent of NO_x, as the increase in oxidizing capacity with NO_x is largely balanced by a decrease in VOC reactivity. Thus, the observed NO_x dependence of HCHO mainly reflects the changing fate of organic peroxy radicals.”

These points appear to contradict two main findings of a paper just out as an accepted preprint in JGR (Valin et al., “The role of OH production in interpreting the variability of CH₂O columns in the Southeast U.S.”). Regarding the first point, Valin et al. state that the feedbacks of P(OH) on CH₂O removal and production do not offset each other, so that CH₂O is not independent of OH. Regarding the second point above, they state: “the yield of CH₂O at low NO_x concentrations is buffered by high-yield RO₂- RO₂ reactions (. . .) in isoprene-rich regions, the influence of NO_x on CH₂O production is primarily due to its feedback on POH, which controls the rate of RO₂ formation, and less so through its effect on the fate of individual RO₂.” It would be worth adding a discussion of these apparent contradictions.

We thank the reviewer for bringing this important paper to our attention. After considering these discrepancies, we discovered an error in our calculation of total RO₂ production from the box model. This error has been resolved, and we now find that RO₂ production does indeed increase with NO_x. Figure 5 and all text has been updated accordingly. We have also added a paragraph comparing our results to those of Valin et al., and an additional panel to Fig. 5 showing the branching ratios for several RO₂ species. Please note that we have also discussed these findings with

the lead author of Valin et al.. The relevant text in Sect. 5 for the above two changes now reads as follows:

"To disentangle these factors, we extract chemical rates from the diel steady-state UWCM simulations discussed in Sect. 5. Figure 5A shows the gross production rates for total peroxy radicals and HCHO as a function of NO_x. Consistent with our earlier discussion, total HCHO production increases by more than a factor of 3 from low to high NO_x. Total RO₂ production increases by a factor of 2 over this same range, driven primarily by increasing OH. The bulk branching ratio β , calculated as the ratio of HCHO and RO₂ production rates, increases from 0.43 to 0.62 (Fig. 5B). This trend is consistent with NO_x-dependent branching ratios of several major HCHO precursors, including isoprene hydroxyperoxy radicals (ISOPO₂) and methyl peroxy radical (Fig. 5B). Based on this analysis, we conclude that enhanced OH production is the main driver for the NO_x dependence of HCHO production, with variations in RO₂ branching playing a lesser (but still important) role.

Using a combination of regional modeling and satellite observations, a recent study by Valin et al. (2016) also examines the drivers of HCHO production. They concur that OH production exerts a controlling influence on HCHO throughout the Southeast U.S. In contrast to our study, however, they assert that changes in RO₂ branching have a negligible effect on the HCHO-NO_x dependence. There are several potential explanations for this discrepancy. First, Valin et al. (2016) derive an "effective branching ratio" that is analogous to the bulk branching ratio in Eqn. (2) but calculated with reference to production of OH rather than RO₂. Many OH sinks do not form RO₂ radicals (e.g. reaction with CO, HCHO, methanol and NO₂) and thus will not make HCHO. The fractional contribution of such reactants to total modeled OH reactivity increases from 36% to 60% over our NO_x range; thus, using P(OH) instead of P(RO₂) to calculate β from Eqn. (2) would effectively normalize out the actual NO_x dependence of the RO₂ branching ratios (Fig. 5B). Second, these two studies use very different photochemical mechanisms. Valin et al. (2016) use a modified version of the lumped Regional Atmospheric Chemistry Mechanism 2 (Browne et al., 2014; Goliff et al., 2013), while our box model uses the explicit MCMv3.3.1 (Jenkin et al., 2015). In Valin et al. (2016), it is stated that decreasing HCHO production from the RO₂ + NO channel is compensated for by increasing production from RO₂ + RO₂ – an effect that we do not observe. Deeper investigation reveals that the rate constant for reaction of ISOPO₂ with HO₂ in RACM2, which is based on work by Paulot et al. (2009b), is a factor of 2 lower than those used in both MCMv3.3.1 and the AM3 mechanism. Thus, our model predicts a significantly larger contribution of RO₂ + HO₂ (which produces negligible HCHO) to the total RO₂ sink. These differences highlight the importance of carefully evaluating chemical mechanisms before using models to interpret in situ and satellite observations."

31599, when discussing the yields of HCHO from isoprene, please be explicit about the units to avoid confusion (here, ppb/ppb aka mol/mol) as some previous work has used carbon-based yields

We have ensured that units appear on all numbers referring to yields.

31601, 12-18: in the Valin et al. paper referenced above, they argue that a steady-state assumption is justified for HCHO but not for isoprene with respect to its emissions. Does this have a significant bearing on the model application here?

We believe that this finding adds validity to our use of a steady-state 0-D box model to calculate HCHO over the Southeast U.S. We are not assuming that isoprene is in steady state, but rather that HCHO is in steady-state with its sources and sinks. Box model isoprene is constrained by observations.

31601, it would aid the interpretation of Fig 4 to discuss the differences between AM3 and UWCM in terms of the isoprene chemistry implemented in each. To what degree could the discrepancies between the two in Fig 4 reflect mechanistic chemical differences? Or is it just the effect of steady-state versus non-steady-state model frameworks?

Though the two models actually agree quite well in Fig. 4, we have considered differences in their mechanisms. We have added the following paragraph to Sect. 5, along with two new supplementary figures (S6-S7).

“The agreement between AM3 and UWCM-MCMv3.3.1 is consistent with how these mechanisms treat first-generation ISOPO₂ radicals (Figs. S6 and S7). Both models use the same rate constants for reactions of ISOPO₂ with NO and HO₂, which comprise the bulk of ISOPO₂ sink. The AM3 mechanism assigns a 12% yield of HCHO to the reaction of ISOPO₂ with HO₂ (Paulot et al., 2009b), while the MCM assumes 100% production of peroxides for this channel. This may explain some of the discrepancy in the prompt yield at low NO_x (Fig. 4A), though neither mechanism is consistent with the current experimental HCHO yield of ~6% HCHO (Liu et al., 2013). There are also two key differences in the minor reaction channels. First, the rate constant for reaction of ISOPO₂ with other RO₂ is an order of magnitude lower in AM3 compared to MCMv3.3.1 (1.54 vs 12 – 16 × 10⁻¹³ cm³ s⁻¹, the latter depending on the ISOPO₂ isomer distribution). This reaction can produce HCHO with yields comparable to that of ISOPO₂ + NO and may be an important source in very-low NO_x regimes. Second, AM3 assumes a constant ISOPO₂ isomer distribution and thus under-predicts the isomerization rate relative to MCMv3.3.1, especially at mid to high NO_x (Fig. S7D). AM3 also includes HCHO and other small oxidized VOC as direct products of isomerization rather than producing hydroperoxyaldehydes and other large products, which influences the timescale of HCHO production and thus the partitioning between prompt and background HCHO. The impact of the RO₂ reaction and isomerization channels on HCHO yields is likely minor but depends significantly on the RO₂/HO₂ ratio (at low NO_x) and on the overall ISOPO₂ lifetime, which affects the ISOPO₂ isomer distribution. For the particular model conditions in Fig. S3B, ISOPO₂ lifetimes for the two mechanisms can differ by as much as 25% at the lowest NO_x values (Fig. S7E). Regardless of these differences, the results shown in Fig. 4 confirm that both the condensed AM3 and explicit MCMv3.3.1 mechanisms perform similarly with regard to overall HCHO production.”

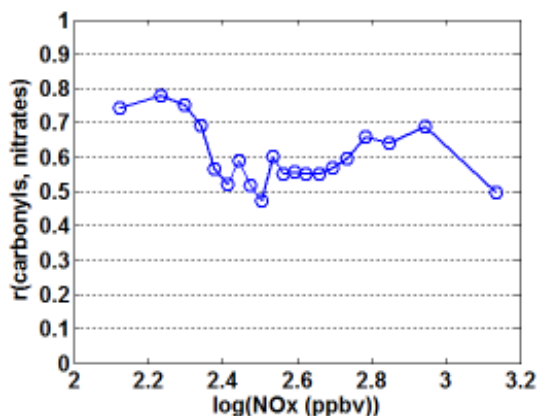
Referee 2

Wolfe and colleagues have analyzed formaldehyde observations made in regions with large isoprene fluxes as a function of NO_x levels. They find that the ‘prompt’ (e.g. within one day) yield of formaldehyde varies with NO_x in a fashion consistent with photochemical theory. Subsequent HCHO formation (e.g. ‘background levels’), however, are larger than can be explained, suggesting that formation from longer-lived organic compounds may not be described accurately by current photochemical theory. Finally, they suggest that in regions with high isoprene emissions, the formation rate of peroxy radicals remains largely constant with NO_x. This is a nice analysis; the manuscript is well written. I suggest publication in ACP following a few suggested modifications / tests.

1. The behavior of the UWCMv2.2 illustrated in Figure S4 suggests that below 200 ppt, RO₂ + RO₂ chemistry is a non-significant contributor to MVK and MACR (especially the latter). Is there support for the importance of RO₂+RO₂ chemistry in the field data? Although not unrelated to point 2 below, I suggest an analysis of the isoprene nitrates (C₅ + C₄ second generation) may be illustrative. If RO₂ + RO₂ becomes a dominant source of MVK+MACR, we anticipate that at low NO_x, the nitrates and carbonyls will no longer be correlated.

Having the best possible estimate for MVK and MACR yields is important as it affects the calculation of initial isoprene and thus the “prompt yield”, so we thank the reviewer for these comments. First, we have recalculated the MVK and MACR yields using MCMv331. In the newer mechanism at low NO_x, the MVK yield increased and the MACR yield decreased.

Regarding the sources of MVK and MACR (and the possible role of RO₂+RO₂), we have looked at the model sources of these compounds for NO values of 20 and 200 ppt (5th and 95th percentiles of observed NO, see green lines above). At 200 pptv NO, ISOP₂ + NO dominates the sources of both, as we expect. At 20 pptv NO, RO₂ + RO₂ comprises 20% of the ISOP_{BO} source (precursor to MVK) and 48% of the ISOP_{DO} source (precursor to MACR). As the reviewer points out here and in item (4) below, this may be less representative of reality due to the fixed OH concentrations in the simulation giving rise to excess RO₂ at low NO_x.

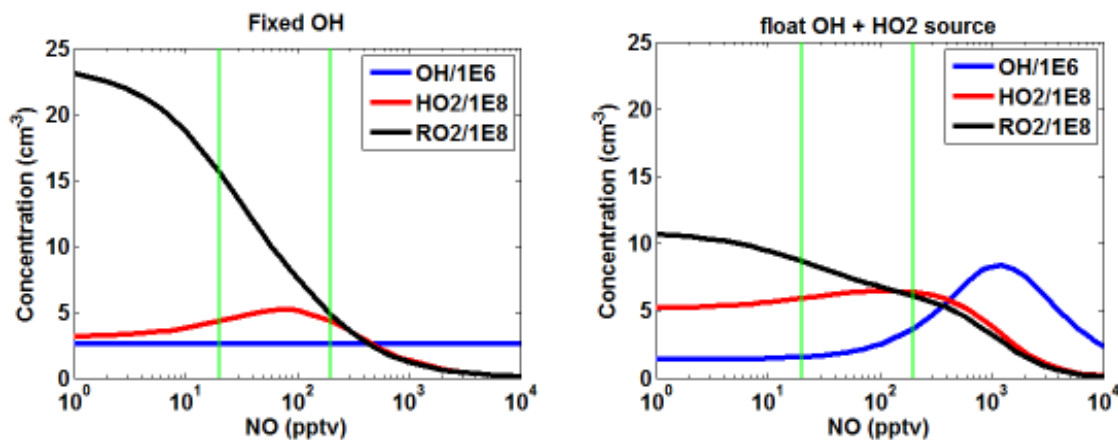


carbonyls here. Assuming that this correlation is driven by the fate of RO₂, this is also consistent

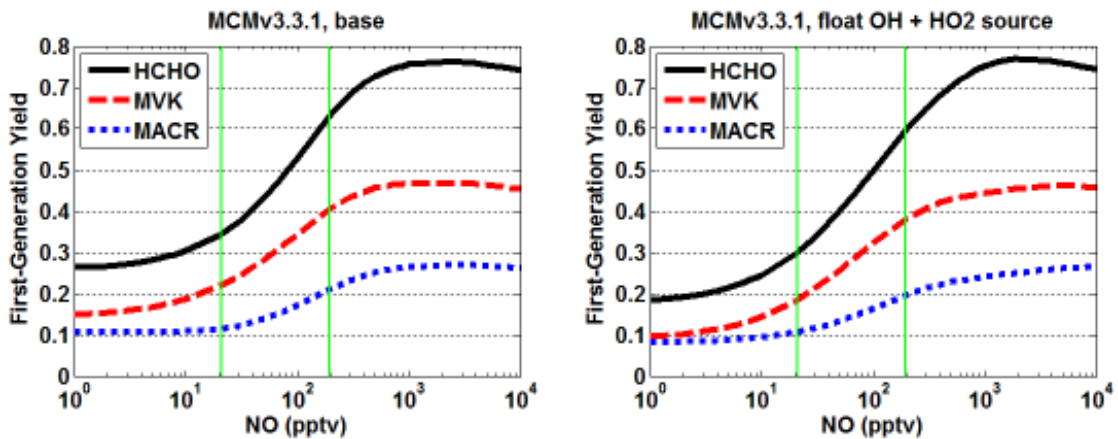
Following the reviewer’s suggestion, we have examined the correlation of MVK+MACR (PTRMS) with isoprene nitrates (UW CIMS, C₅H₉O₄N₁+C₄H₇O₅N₁) as a function of NO_x. Here we use the same procedure as that used for the linear fitting shown in Fig. 3 of the main text. The figure to the left shows the correlation coefficient for these two observations when grouped by NO_x. The two measurements are most well correlated at low NO_x, consistent with RO₂+RO₂ not being a dominant source of

with the MVK+MACR observations NOT having a significant interference from ISOPOOH (discussed further below); if ISOPOOH were a significant contributor to the MVK+MACR signal, we would expect this correlation to degrade at lower NO_x where ISOPO₂ + HO₂ is favored.

In light of these issues, we have modified the yield simulations to better represent the distribution of RO₂ sinks by allowing OH to be determined by the conditions in the simulation. In this case, these conditions are taken from NOAA P-3 observations over the SOAS Centreville site on June 10, 2013 (CO = 120 ppbv, O₃=50 ppbv, SZA = 10 degrees, RH = 75%). In addition, we add a source of HO₂, equivalent to photolysis of 5 ppbv HCHO, to compensate for HO₂ sources not included in pseudo-chamber simulation. The figures below show RO_x concentrations in the old and new simulations (both using MCMv3.3.1). At 20 pptv NO, OH and RO₂ decrease by 40% and HO₂ increases by 40%. OH and HO₂ concentrations are comparable to those observed during SOAS, and the HO₂/RO₂ ratio is within the range of values calculated in the full steady-state simulation.



This results in a general lowering of the yield curves, though the effects are relatively minor over the range of NO_x values relevant to this study (vertical green lines denote 5th and 95th percentiles of data).



We believe that this is the best possible representation of the NO-dependent yields that we can gain with the available information, and we use the “MCMv3.3.1 + floatOH + HO₂ source” yields in the

subsequent calculation of initial isoprene. We have also added a plot of ROx concentrations to Fig. S3. Please note that, despite these modifications, our main results (Figures 3 and 4) are essentially unchanged.

Is the fate of the RO2s different between AM3 and UWCM? A figure in the supplement showing the branching ratios vs NOx would be welcome.

Yes. Please see Figures S7 and S8 in the SI, as well as our above response to Referee 1 on this subject.

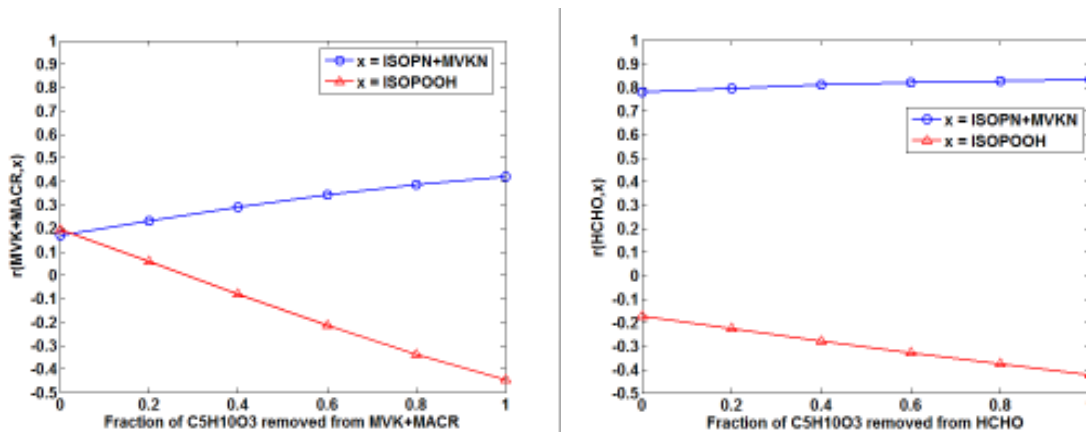
2. I am surprised that the NOAA PTRMS would not convert ISOPOOH to MVK/MACR. Has this been verified with standards of ISOPOOH? Are there differences between the drift tube used by the European groups and NOAA that might explain why there is minimal conversion in the NOAA CIMS? I find the analysis presented in S1 and S2 to be less than compelling. In the SEAC4RS data, ISOPOOH is anticorrelated with MVK+MACR (while IEPOX is uncorrelated) as might be expected from the photochemical mechanism. Does C5H10O3 show such an anticorrelation (From S1 it appears not)? During the Caltech FIXCIT experiments, the Colorado State I- CIMS was found to be more sensitive to IEPOX than ISOPOOH. Is that also the case for UW I- CIMS? If so, perhaps the analysis described in the supplement is less compelling of a test. In the SEAC4RS data, we find that $(m/z79 - 0.8*ISOPOOH)$ is very highly correlated with ISOPN+MVKN while the correlation with $m/z79$ alone is much more scattered. We have interpreted that to suggest that the conversion is high. In light of the substantial non-NO production of MVK+MACR suggested by S4, perhaps this may be a fortuitous result. It would be interesting to see a similar analysis for SENEX.

The NOAA PTRMS has not been tested for interferences with an ISOPOOH standard, thus we cannot definitively rule out an interference or develop a correction factor. We do not, however, feel that this is cause to discard the data as unusable; moreover, our key findings are robust against even a substantial interference, as discussed further below. First, we note that recent lab experiments have confirmed a low conversion rate (<5% of ISOPOOH) for the HCHO instrument used during SENEX, and we have added a reference to the appropriate paper (St. Clair et al., in preparation, 2016) in the text.

Regarding the NOAA PTRMS: The NOAA and European (Wisthaler group) instruments are both derived from IONICON and thus likely have similar drift tubes, though the inlet systems may be different. The NOAA inlet is 1/8" OD silcosteel, heated to ~30C, with a typical residence time of <1 second from ambient to instrument. To our knowledge, there is no published work yet that has sufficiently characterized the details of ISOPOOH conversion in these instruments, and it is not clear how the conversion might depend on flow rates, electric fields, etc. Thus, such comparisons should be viewed with caution.

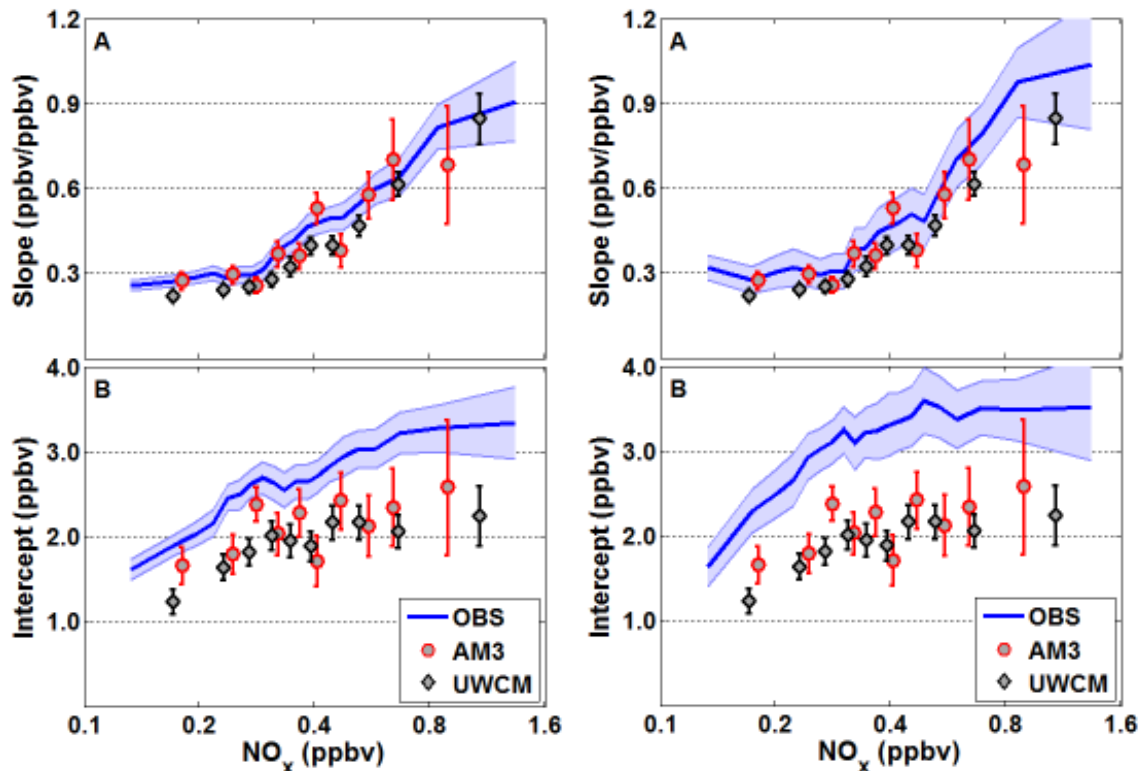
Regarding the UW-CIMS: For the C5H10O3 mass, the UW-CIMS as flown on SENEX is ~8.5 times more sensitive to ISOPOOH than to IEPOX (B. Lee, personal communication, 2016). During SEAC4RS, the Caltech triple-quad observed, on average, equal amounts of ISOPOOH and IEPOX in the SEUS. Thus, we expect that this mass is primarily representative of ISOPOOH.

Regarding correlation of MVK+MACR with other oxidation products: We assume here that the reviewer intended to write m/z 71 (the PTRMS mass for MVK+MACR) rather than m/z 79 in the above comment. For a clear view of the NO_x dependence of RO₂ fates, we look at a single SENEX flight on 20130616 in the Atlanta area. In power plant plumes, we typically find that nitrates are elevated and ISOPOOH is depleted; MVK+MACR can go up or down, but the variability and limited time resolution of this signal makes it difficult to distinguish clear trends. We examined the correlation coefficients between MVK+MACR and both nitrates and ISOPOOH, looking at how these change as fractions of the C₅H₁₀O₃ signal are subtracted from the PTRMS m/z 71 signal.



The plot on the left shows that the correlation with nitrates increases while that with ISOPOOH decreases, as the reviewer noted. As a check, we performed this same calculation with HCHO. Here we find similar trends, though somewhat less in magnitude than for the MVK+MACR case. Also, the trend in $r(\text{MVK+MACR}, \text{ISOPN+MVKN})$ would continue to increase even when subtracting more than 100% of the C₅H₁₀O₃ signal from m/z 71. Thus, it is not clear that such correlations are an unbiased diagnostic of potential interferences.

We agree that Figures S1 – S3 are not compelling and have removed them from the supplement. Instead, we have opted for a more careful comparison of the iWAS and PTR-MS to get some handle on the potential for an interference in either measurement. Through this analysis (see text below), we surmise that the conversion efficiency of ISOPOOH in the PTR-MS is likely no more than 50%. As a sensitivity test, apply such a correction and rerun all calculations with these new MVK+MACR concentrations. The plots below compare Figure 4 from the main text using MVK+MACR as observed (left) and with this correction (right). There is clearly some increase in the variability of observation-based slopes and intercepts, and the intercept increases faster at mid-NO_x values; however, the overall trends are robust.



To summarize: we cannot conclusively rule out ISOPOOH conversion in the PTRMS and iWAS instruments. To our knowledge, there is also no way to unambiguously quantify such interferences using the available observations. Furthermore, our key conclusions are robust against a substantial assuming conversion rate of 50%. We have made a number of changes to the text, including deleting section S1 and Figures S1-S3, adding two new figures to the supplement (now S1 and S2), and adding substantial text to Section 2 of the main paper, which reads as follows.

“Measurements of MVK and MACR may include a positive bias from conversion of isoprene hydroxyhydroperoxides (ISOPOOH) on hot metal surfaces in the sampling system (Liu et al., 2013; Rivera-Rios et al., 2014). ISOPOOH mixing ratios up to 2 ppbv were observed by the University of Washington Iodide chemical ionization mass spectrometer during SENEX. Neither the NOAA PTR-MS nor the iWAS have been tested for this interference with an ISOPOOH standard, thus we cannot definitively rule out such artifacts or develop a correction factor. To our knowledge, it is not yet clear how the putative interference depends on instrument configuration (flow rates, electric fields, etc.). Thus, caution is warranted when comparing the SENEX systems to similar, but not identical, instruments. Theoretically, this mechanism could give rise to an analogous artifact in HCHO observations. Recent laboratory tests, however, indicate that the ISOPOOH-to-HCHO conversion efficiency in ISAF is less than 5% (St. Clair et al., 2016).

We cannot unambiguously quantify such interferences using observations alone, but we can gain some insight from comparing PTR-MS and iWAS data. On average, iWAS observations of MVK+MACR are 40% higher than those from the PTR-MS (Figs. S1 and S2), suggesting a systematic

bias in one or both measurements. Both instruments were calibrated using the same gas standards, and the two techniques agree well for other species such as isoprene (Lerner et al., 2016; Warneke et al., 2016), so a calibration error is unlikely. Production of oxygenated VOC in ambient air samples collected and aged in stainless steel canisters cannot be ruled out. For example, enhancements in MVK (above the 20% uncertainty) have been observed in canisters after aging over ~11 days (Lerner et al., 2016), though this is significantly longer than typical turn-around times for SENEX. To evaluate the potential for ISOPOOH conversion to explain this discrepancy, we plot the ratio and difference of the PTR-MS and iWAS measurements as a function of ISOPOOH in Fig. S2. While the ratio is essentially constant (iWAS/PTR-MS ~1.43), the absolute difference exhibits a strong correlation with ISOPOOH ($r^2 = 0.43$). The slope of this relationship implies that a conversion of 50% of ISOPOOH to MVK and/or MACR in the iWAS system would explain the difference in the two measurements. Correcting total iWAS MVK + MACR for such an artifact reduces the slope of the iWAS-PTR-MS correlation from 1.48 to 1.24 (Fig. S1B). In practice, we cannot apply such a correction to the speciated iWAS observations as the conversion efficiency may be different for each isomer. This result does not exclude the possibility of an artifact in the PTR-MS measurement, though it does suggest an upper limit ISOPOOH conversion efficiency of 50% for the PTR-MS (in which case, the conversion would be 100% for the iWAS). The analysis presented in Sections 3 and 4 primarily relies on PTR-MS data due to its greater temporal coverage. Even when applying a 50% ISOPOOH correction to the PTR-MS data, we find only minor differences in our key results; thus, we use the data without correction.”

3. The update to the isoprene chemistry in MCM (used in UWCMv2.2) has now been published in ACP as version 3.3.1. I suggest updating UWCMv.2.2 to this version which is now the standard MCM.

We have used MCMv3.3.1 in both the calculation of product yields and in the full diel steady state simulation. All figures and text have been updated. The most notable impact of this mechanism is that the theoretical isoprene daughter/parent relationship now falls directly on the observed relationship in Fig. 2. Our overall conclusions, however, are unaffected.

4. Related to 1, the analysis shown in S4 has the production rate is ISOPOO constant across NO_x. I expect that the fate of these RO₂s is sensitive to the rate of their production in the low NO regime. An analysis exploring this sensitivity would be welcome.

Please see the above discussion of item (1). By altering the yield simulation to more faithfully represent atmospheric conditions, we hope that this issue has been addressed and further sensitivity tests are unnecessary.

Small points:

1. Pg. 31589; In 5, add ‘photochemical’ before mechanism

Done.

2. Pg. 31589; In 22, does ‘increase in oxidizing capacity’ here just mean [OH]? If so, please substitute.

This text has been altered following reviewer 1's comments.

3. Pg. 31590; In 25. Such models are also needed to provide vertical distribution of HCHO as the averaging kernel of the remote sensed columns is strongly altitude dependent.

This sentence has been modified to read as follows: *“Typically, a chemical transport model is employed both to supply a priori HCHO vertical distributions for satellite retrievals (González Abad et al., 2015) and to relate HCHO column concentrations to isoprene emission strength.”*

4. Pg. 31594; In 24. The focus here is solely on daytime chemistry. I suggest a few words (perhaps with use of the AM3) to demonstrate the lack of sensitivity to nighttime chemistry in your conclusions.

We have added the following text to the bottom of this paragraph: *“HCHO, MVK and MACR are also high-yield products of isoprene ozonolysis (Atkinson and Arey, 2003), but as noted above this reaction is relatively slow. Nighttime oxidation of isoprene by NO₃ radical is also likely a negligible source of these carbonyls (Brown et al., 2009). Yields are small (Atkinson and Arey, 2003; Kwok et al., 1996), and the lifetimes of these compounds is sufficiently short that any nighttime production should not influence the midday considered here.”*

5. Pg. 31602; In 8-10. A brief description of just how different the isoprene chemistry is between AM3 and the UW model would be helpful. Are they really that different (for this chemistry)?

Please see our above response to Reviewer 1 on this topic.

Referee 3

Wolfe et al. introduce airborne observations of formaldehyde and isoprene, a main precursor for formaldehyde. Utilizing box and global models, they examine formaldehyde yields in a wide NO_x spectrum. A comprehensive observational dataset on NOAA P-3 during the SENEX campaign is utilized to observationally constrain the box model. The presented quantitative information about formaldehyde background concentrations and formation rates/yields could be used for critical information in interpreting satellite datasets as the authors argued. As a constellation of geostationary satellites will be launched for air composition monitoring, this work will provide highly valuable constraints to retrieve isoprene emission rates using an inverse modelling scheme. I recommend publishing this manuscript in ACP after the considerations of a couple of suggestions

1) Page 31593: As the ISOPOOH interferences on MVK and MACR in the conventional analytical techniques are still controversial and relatively new, I would recommend including the justification for the conclusion of negligible ISOPOOH interferences on PTR-MS and whole air sample-GC-MS techniques in the main text rather than in the supplementary material

We have heavily modified our discussion of this topic, and all the relevant discussion is now included in the main text. Please see our response to Reviewer #2 on this subject.

2) It would be helpful to discuss about what is the implications of the recently reported faster than expected dry deposition rates (e.g. Nguyen et al. 2015 PNAS) in this study.

We do not expect the findings of Nguyen et al. (2015) to have a significant impact on our work. Faster deposition for oxidized VOC would potentially remove some precursors of HCHO, and if this is not accurately represented in AM3 or UWCM then we would potentially expect some over-prediction of HCHO. From Figure 4, however, it is evident that both models are missing HCHO. Moreover, the photochemical lifetimes of most of the compounds discussed in Nguyen et al. are sufficiently short that deposition should be a minor contribution to their sink.

1 **Formaldehyde production from isoprene oxidation across**
2 **NO_x regimes**

3 **G. M. Wolfe^{1,2}, J. Kaiser³, T. F. Hanisco², F. N. Keutsch⁴, J. A. de Gouw^{5,6}, J. B.**
4 **Gilman^{5,6}, M. Graus^{5,6,*^a}, C. D. Hatch⁷, J. Holloway^{5,6}, L. W. Horowitz⁸, B. H.**
5 **Lee⁹, B. M. Lerner^{5,6}, F. Lopez-Hilfiker^{9,b}, J. Mao^{8,11}, M. R. Marvin¹⁰, J. Peischl^{5,6},**
6 **I. B. Pollack^{5,6}, J. M. Roberts⁶, T. B. Ryerson⁶, J. A. Thornton⁹, P. R. Veres^{5,6}, C.**
7 **Warneke^{5,6}**

Formatted: Superscript

8 [1]Joint Center for Earth Systems Technology, University of Maryland Baltimore County,
9 Baltimore, MD, USA

10 [2]Atmospheric Chemistry and Dynamics Laboratory, NASA Goddard Space Flight Center,
11 Greenbelt, MD, USA

12 [3]Department of Chemistry, University of Wisconsin-Madison, Madison, WI, USA

13 [4]School of Engineering and Applied Sciences and Department of Chemistry and Chemical
14 Biology, Harvard University, Cambridge, MA, USA

15 [5]Cooperative Institute for Research in Environmental Sciences, University of Colorado
16 Boulder, Boulder, CO, USA

17 [6]Chemical Sciences Division, NOAA Earth System Research Laboratory, Boulder, CO,
18 USA

19 [7]Department of Chemistry, Hendrix College, Conway, AR, USA

20 [8]NOAA Geophysical Fluid Dynamics Laboratory, Princeton, NJ, USA

21 [9]Department of Atmospheric Sciences, University of Washington, Seattle, WA, USA

22 [10]Department of Chemistry, University of Maryland, College Park, MD, USA

23 [11]Program in Atmospheric and Oceanic Sciences, Princeton University, Princeton, NJ

24 ^{*[a]}Now at Institute of Atmospheric and Cryospheric Sciences, Innsbruck University, Austria

25 [b]Now at Laboratory of Atmospheric Chemistry, Paul Scherrer Institut, 5232 Villigen,
26 Switzerland

27 Correspondence to G. M. Wolfe (glenn.m.wolfe@nasa.gov)

1

2 **Abstract**

3 The chemical link between isoprene and formaldehyde (HCHO) is a strong, non-linear
4 function of NO_x ($= \text{NO} + \text{NO}_2$). This relationship is a linchpin for top-down isoprene emission
5 inventory verification from orbital HCHO column observations. It is also a benchmark for
6 overall photochemical mechanism performance with regard to VOC oxidation. Using a
7 comprehensive suite of airborne *in situ* observations over the Southeast U.S., we quantify
8 HCHO production across the urban-rural spectrum. Analysis of isoprene and its major first-
9 generation oxidation products allows us to define both a “prompt” yield of HCHO (molecules
10 of HCHO produced per molecule of freshly-emitted isoprene) and the background HCHO
11 mixing ratio (from oxidation of longer-lived hydrocarbons). Over the range of observed NO_x
12 values (roughly 0.1 – 2 ppbv), the prompt yield increases by a factor of 3 (from 0.3 to 0.9
13 ppbv ppbv⁻¹), while background HCHO increases by ~~more than~~ a factor of 2 (from 1.56 to 3.3
14 ppbv). We apply the same method to evaluate the performance of both a global chemical
15 transport model (AM3) and a measurement-constrained 0-D ~~chemical~~steady state box model.
16 Both models reproduce the NO_x dependence of the prompt HCHO yield, illustrating that
17 models with updated isoprene oxidation mechanisms can adequately capture the link between
18 HCHO and recent isoprene emissions. On the other hand, both models under-estimate
19 background HCHO mixing ratios, suggesting missing HCHO precursors, inadequate
20 representation of later-generation isoprene degradation and/or under-estimated hydroxyl
21 radical concentrations. ~~Moreover, we find that the total organic peroxy radical production rate
22 is essentially independent of NO_x , as the increase in oxidizing capacity with NO_x is largely
23 balanced by a decrease in VOC reactivity. Thus, the observed NO_x dependence of HCHO
24 mainly reflects the changing fate of organic peroxy radicals~~Detailed process rates from the
25 box model simulation demonstrate a 3-fold increase in HCHO production across the range of
26 observed NO_x values, driven by a 100% increase in OH and a 40% increase in branching of
27 organic peroxy radical reactions to produce HCHO.

28

29 **1 Introduction**

30 Formaldehyde (HCHO) is a ubiquitous byproduct of volatile organic compound (VOC)
31 oxidation. While methane is the principal HCHO precursor in remote regions, larger VOC are
32 the main source over continents. HCHO is also directly emitted via biomass burning (Lee et

1 al., 1997), fossil fuel combustion (Luecken et al., 2012), natural gas flaring (Knighton et al.,
2 2012), ethanol refining (de Gouw et al., 2015), possibly vegetation (DiGangi et al., 2011) and
3 agricultural activity (Kaiser et al., 2015a), but chemical production dominates the global
4 budget (Fortems-Cheiney et al., 2012). Photolysis and reaction with OH destroy HCHO with
5 a characteristic lifetime of several hours during midday, implying that the HCHO abundance
6 reflects recent ~~hydrocarbon~~VOC oxidation.

7 Globally, isoprene is the main precursor of near-surface HCHO. A highly reactive
8 diene emitted by vegetation, isoprene comprises roughly one third of all non-methane VOC
9 emissions (Guenther et al., 2012). Oxidation of isoprene in the presence of nitrogen oxides
10 ($\text{NO}_x = \text{NO} + \text{NO}_2$) stimulates the production of ozone (Trainer et al., 1987) and organic
11 aerosol precursors (Xu et al., 2015), impacting air quality and climate in many continental
12 regions. Biogenic emission inventories struggle to accurately represent the spatiotemporal
13 variability of isoprene emissions, with model-measurement discrepancies and differences
14 among emission inventories approaching a factor of 2 or more (Carlton and Baker, 2011;
15 Warneke et al., 2010). Such differences directly impact predicted ozone and aerosol
16 distributions (Hogrefe et al., 2011).

17 Numerous studies have applied satellite-based HCHO column observations as a top-
18 down constraint on isoprene emissions (see Kefauver et al. (2014) for a review). ~~Typically, a~~
19 ~~chemical transport model is employed to relate HCHO column concentrations to isoprene~~
20 ~~emission strength.~~Typically, a chemical transport model is employed both to supply a priori
21 HCHO vertical distributions for satellite retrievals (González Abad et al., 2015) and to relate
22 HCHO column concentrations to isoprene emission strength. Early studies utilized linear
23 steady-state relationships (Palmer et al., 2003), while recent computational advances have
24 permitted full inversions that more fully account for transport, multiple sources and varying
25 chemical regimes (Fortems-Cheiney et al., 2012). Such techniques have informed isoprene
26 emission inventories in North America (Abbot et al., 2003; Millet et al., 2008; Millet et al.,
27 2006; Palmer et al., 2006; Palmer et al., 2003), South America (Barkley et al., 2013; Barkley
28 et al., 2008), Europe (Curci et al., 2010; Dufour et al., 2009), Africa (Marais et al., 2012),
29 Asia (Fu et al., 2007; Stavrou et al., 2014), and globally (Fortems-Cheiney et al., 2012;
30 Shim et al., 2005; Stavrou et al., 2009). Future geostationary observations, such as the
31 NASA Tropospheric Emissions: Monitoring of Pollution (TEMPO,
32 <http://science.nasa.gov/missions/tempo/>) mission, will permit an even more detailed

1 investigation of the spatial and temporal variability of isoprene emissions and other VOC
2 sources.

3 Chemistry dictates the relationship between HCHO columns and underlying isoprene
4 emissions. Many of the above-listed studies apply 0-D box model calculations to evaluate the
5 yield of HCHO from isoprene as a function of oxidation time, NO_x regime and chemical
6 mechanism. In all cases, it is found that NO_x enhances both the production rate and ultimate
7 yield of HCHO. Slower production at lower NO_x can lead to “smearing,” whereby HCHO
8 production is displaced relative to the isoprene source. Palmer et al. (2003) define a
9 characteristic smearing length scale, which can range from 10 to 100 km or more.
10 Furthermore, accumulation of oxygenated VOC over multiple generations of isoprene
11 degradation can contribute to substantial background HCHO production, which is not directly
12 linked with fresh isoprene emissions. Long-lived primary anthropogenic or biogenic
13 emissions, like methane and methanol, can also contribute to this background. Background
14 column concentrations are typically on the order of $5 \times 10^{15} \text{ cm}^{-2}$, equating equal to 20% or
15 more of the isoprene-driven HCHO column enhancement (Barkley et al., 2013; Millet et al.,
16 2006). A wave of recent theoretical (Peeters et al., 2014; Peeters and Müller, 2010; Peeters et
17 al., 1999), laboratory (Crouse et al., 2012; Crouse et al., 2011; Paulot et al., 2009a; Paulot
18 et al., 2009b) and field (Mao et al., 2012) research has highlighted shortcomings in low-NO_x
19 isoprene oxidation schemes. Such issues translate directly into top-down emission estimates;
20 for example, Marais et al. (2012) report an uncertainty of 40% in OMI satellite-derived
21 African isoprene emissions at high-NO_x and 40-90% at low-NO_x. Coarse resolution of
22 averaged satellite observations and model simulations (typically $1^\circ \times 1^\circ$ or more) has partly
23 mitigated these problems in prior work, as variability in NO_x-dependent smearing and
24 background production is averaged out. A more careful treatment will be needed to harness
25 the enhanced resolution of near-future orbital observations (e.g., $8 \times 4.5 \text{ km}^2$ for TEMPO),
26 especially since these measurements will include diurnal variability.

27 Here, we use a comprehensive set of *in situ* observations to quantify the impact of NO_x
28 on the isoprene-HCHO chemical link. Using isoprene and its unique first-generation products,
29 we segregate HCHO into two categories. The first, defined as “prompt” HCHO, is produced
30 from fresh isoprene emissions (on a timescale of less than a day) and retains the signature of
31 isoprene emission source strength. The second category is “background” HCHO stemming
32 from oxidation of longer-lived isoprene oxidation products and other VOC. We examine the

1 NO_x dependence of both quantities. Applying the same method to 0-D and global model
2 simulations, we evaluate the ability of current chemical mechanisms to replicate the observed
3 trends. Box model results are also used to elucidate the mechanistic underpinnings of the NO_x
4 influence on HCHO production.

5

6 **2 SENEX Observations**

7 The Southeast Nexus (SENEX) mission was an airborne campaign designed to examine the
8 interaction of natural and anthropogenic emissions- (Warneke et al., 2016). During June and
9 July of 2013, the NOAA WP-3D aircraft logged ~~14~~about 120 flight hours over ~~18~~20 research
10 flights in a range of environments throughout the Southeast United States, including urban
11 centers, power plant plumes, natural gas extraction regions, agricultural areas and forests. The
12 payload included a suite of gas- and particle-phase instrumentation- (Warneke et al., 2015).
13 Here we utilize observations of HCHO, isoprene, methyl vinyl ketone (MVK), methacrolein
14 (MACR), NO and NO₂. HCHO was measured at 1 Hz by the NASA In Situ Airborne
15 Formaldehyde (ISAF) instrument, which ~~relies on~~utilizes the laser-induced fluorescence
16 technique and has an accuracy of ±10% (Cazorla et al., 2015). Isoprene, MVK and MACR
17 were measured by both a quadrupole proton transfer reaction mass spectrometer (PTR-MS)
18 and the NOAA improved whole-air sampler (iWAS) with offline gas chromatography. The
19 PTR-MS (de Gouw and Warneke, 2007) has a stated accuracy of 20% and sequentially
20 sampled masses for isoprene (m/z +69) and the sum of MVK and MACR (m/z +71) for 1 s
21 each with a duty cycle of 14 s. The iWAS (~~Lerner et al., 2015~~)(Lerner et al., 2016) collected
22 72 canister samples each flight, which were analyzed offline with gas chromatography – mass
23 spectrometry 3-4 days post-flight. iWAS measurement uncertainty is 20% for speciated MVK
24 and MACR and 27% for isoprene. NO and NO₂ were measured at 1 Hz via
25 chemiluminescence coupled with a photolytic NO₂ converter (Pollack et al., 2010; Ryerson et
26 al., 1999) with an accuracy of 5%. Data are filtered to include only daytime boundary layer
27 conditions (solar zenith angle < 60°, radar altitude < 1 km). Influence from biomass burning
28 (acetonitrile > 210 pptv and CO > 300 ppbv) is also removed. This procedure, along with the
29 disjunct nature of the PTR-MS measurement, excludes 50% of all fast (1 Hz) data. After
30 accounting for ~~missing data~~gaps, we retain 8435 1 Hz data points and 81 iWAS samples.

31 Measurements of MVK and MACR ~~can~~may include a positive bias from conversion of
32 isoprene hydroxyhydroperoxides (ISOPOOH) on hot metal surfaces in the sampling system

1 (Liu et al., 2013; Rivera-Rios et al., 2014). ISOPOOH mixing ratios up to 2 ppbv were
2 observed by the University of Washington Iodide high-resolution time-of-flight chemical
3 ionization mass spectrometer during SENEX. Neither the NOAA PTR-MS nor the iWAS
4 have been tested for this interference with an ISOPOOH standard, thus we cannot definitively
5 rule out such artifacts or develop a correction factor. To our knowledge, it is not yet clear how
6 the putative interference depends on instrument configuration (flow rates, electric fields, etc.).
7 Thus, caution is warranted when comparing the SENEX systems to similar, but not identical,
8 instruments. Theoretically, this mechanism could give rise to an analogous artifact in HCHO
9 observations. ~~ISOPOOH mixing ratios of roughly 0 to 2 ppbv were observed during SENEX~~
10 ~~(see supporting information (SI)). It is difficult to~~Recent laboratory tests, however, indicate
11 ~~that the ISOPOOH-to-HCHO conversion efficiency in ISAF is less than 5% (St. Clair et al.,~~
12 ~~2016).~~

13 We cannot unambiguously quantify the magnitude of any such interference from
14 field ISOPOOH artifact using observations alone. Based on a comparison to, but we can gain
15 some insight from comparing PTR-MS and iWAS data. On average, iWAS observations of
16 MVK+MACR are ~40% higher than those from the PTR-MS (Figs. S1 and S2), suggesting a
17 systematic bias in one or both measurements. Both instruments were calibrated using the
18 same gas standards, and the two techniques agree well for other species such as isoprene
19 oxidation products and (Lerner et al., 2016; Warneke et al., 2016), so a calibration error is
20 unlikely. Production of oxygenated VOC in ambient air samples collected and aged in
21 stainless steel canisters cannot be ruled out. Enhancements in MVK and MACR (above the
22 20% uncertainty) have been observed in canisters after aging over ~11 days (Lerner et al.,
23 2016), though this is significantly longer than typical turn-around times for SENEX. To
24 evaluate the potential for ISOPOOH conversion to 0-D box model results (SI), we argue that
25 such artifacts are negligibly small in the PTR-MS and ISAF explain this discrepancy, we plot
26 the ratio and difference of the PTR-MS and iWAS measurements as a function of ISOPOOH
27 in Fig. S2. While the ratio is essentially constant (iWAS/PTR-MS ~1.43), the absolute
28 difference exhibits a strong positive correlation with ISOPOOH ($r^2 = 0.43$). The slope of this
29 relationship implies that a conversion of 50% of ISOPOOH to MVK and/or MACR in the
30 iWAS system would explain the difference in the two measurements. Correcting total iWAS
31 MVK+MACR for such an artifact reduces the slope of the iWAS-PTR-MS correlation from
32 1.48 to 1.24 (Fig. S1B), bringing agreement to well with combined measurement
33 uncertainties. In practice, we cannot apply such a correction to the speciated iWAS

Formatted: Indent: First line: 0.49"

Formatted: Strong

Formatted: Strong

Formatted: Strong

1 observations ~~for SENEX. We cannot rule out a potential positive bias in the iWAS MVK~~
2 ~~measurement; nonetheless, as we show below, the correspondence between observed MVK~~
3 ~~and MACR mixing ratios is consistent with our current understanding of isoprene oxidation~~
4 ~~as the conversion efficiency may be different for each isomer. This result does not exclude the~~
5 ~~possibility of an artifact in the PTR-MS measurement, though it does suggest an upper limit~~
6 ~~ISOPOOH conversion efficiency of 50% for the PTR-MS (which would imply a conversion~~
7 ~~of 100% for the iWAS). The analysis presented in Sections 3 and 4 primarily relies on PTR-~~
8 ~~MS data due to its greater temporal coverage. Our key conclusions are not impacted by a 50%~~
9 ~~ISOPOOH correction to the PTR-MS data, thus we use the data without correction.~~

10 SENEX sampled a wide spectrum of chemical regimes (Figure 1). For the daytime
11 boundary-layer observations presented here, maximum 1 Hz isoprene and NO mixing ratios
12 respectively reach 8.1 and 95 ppbv, while minima are less than a few pptv. The distributions
13 of both isoprene and NO observations are approximately log-normal (top and right panels of
14 Fig. 1), peaking at 1.5 ppbv and 50 pptv, respectively. Though these distributions may be
15 biased towards areas of urban influence, the range of environments encountered during
16 SENEX is representative of the Southeast U.S. summertime boundary layer. The long tail at
17 the low end of the isoprene distribution is mostly associated with regions lacking significant
18 tree cover, ~~notably Illinois and Indiana,~~ where isoprene emissions are lower, ~~notably Illinois~~
19 ~~and Indiana.~~ The NO distribution spans four orders of magnitude (< 10 to $\sim 10^4$ pptv), over
20 which radical chemistry changes markedly. At NO mixing ratios of a few hundred pptv or
21 more, organic peroxy radicals (RO_2) react mostly with NO. At low NO (10's of pptv or less),
22 reaction with HO_2 , other RO_2 and isomerization dominate the RO_2 fate. The bulk of the NO
23 distribution lies in a transition region for radical chemistry, making this dataset ideal for
24 probing the anthropogenic influence on biogenic VOC oxidation.

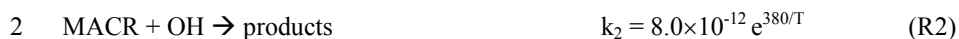
25 HCHO mixing ratios (color shading in Fig. 1) range from 0.8 to 14 ppbv with a mean
26 ~~value~~ of 4.3 ppbv. HCHO is most abundant in regions where both isoprene and NO_x are
27 elevated. High NO_x is often accompanied by increased concentrations of anthropogenic VOC;
28 however, constrained box-model calculations demonstrate that isoprene is the dominant
29 HCHO precursor even in these cases (Sect. 5). ~~Thus, chemistry~~ Thus, changes in radical
30 cycling and partitioning (and not co-variance of NO_x and anthropogenic VOC) drives the
31 observed NO_x dependence of HCHO abundance.

32

1 3 Linking Observed and Emitted Isoprene

2 The isoprene photochemical cascade is a multi-step process. Isoprene oxidation is initiated
3 [by](#) reaction with the hydroxyl radical (OH), ozone, or the nitrate radical (NO₃). In the
4 Southeast U.S., typical daytime levels for OH, ozone and NO₃ are $4 \times 10^6 \text{ cm}^{-3}$, 50 ppbv and
5 0.1 pptv, respectively (OH and NO₃ are estimated from median box model output, see Sect.
6 5). The corresponding isoprene lifetimes at 298K are 0.7 h, 17 h and 160 h, respectively.
7 Thus, reaction with OH typically constitutes 95% or more of the total daytime isoprene sink
8 in this environment. Addition of OH and reaction with O₂ generates one of several isoprene
9 hydroperoxy radicals (ISOPO₂). ISOPO₂ isomers interconvert rapidly due to reversible O₂
10 addition (Peeters et al., 2009) but are eventually destroyed via reaction with NO, hydroperoxy
11 radical (HO₂), other organic peroxy radicals (RO₂) or isomerization. Most branches have the
12 potential to produce HCHO, with varying yields. The laboratory-derived first-generation
13 HCHO yield from the NO pathway is ~0.6 (Atkinson and Arey, 2003), though this value may
14 be less representative of the real atmosphere due to the very high isoprene concentrations (and
15 very short RO₂ lifetimes) in early chamber experiments. The first-generation yield from the
16 HO₂ pathway is ~0.06 (Liu et al., 2013). Isomerization chemistry is less well understood; the
17 1,5-H-shift is believed to produce HCHO with a unity yield, while the much faster 1,6-H-shift
18 should not produce any HCHO (da Silva et al., 2010; Fuchs et al., 2013; Peeters et al., 2014;
19 Peeters and Müller, 2010; Peeters et al., 2009). Regardless of the specific pathway, MVK or
20 MACR are always co-produced with HCHO in the first generation. HCHO is also generated
21 in subsequent chemistry, but on a longer timescale and from a much larger suite of precursors.
22 For example, the OH lifetimes of MACR and MVK are respectively 3.5 and 5 times longer
23 than that of isoprene. [HCHO, MVK and MACR are also high-yield products of isoprene
24 ozonolysis \(Atkinson and Arey, 2003\), but as noted above this reaction is relatively slow.
25 Nighttime oxidation of isoprene by NO₃ radical is also likely a negligible source of these
26 carbonyls \(Brown et al., 2009\). Yields are small \(Atkinson and Arey, 2003; Kwok et al.,
27 1996\), and the lifetimes of MVK, MACR and HCHO are sufficiently short that any nighttime
28 production should not influence the midday observations considered here.](#)

29 Boundary layer composition reflects a mixture of emissions with various degrees of
30 photochemical processing. To isolate the impact of “fresh” isoprene emissions, we exploit the
31 relatively simple chemistry of MVK and MACR, which are produced via isoprene [\(ISOP\)](#)
32 oxidation and lost primarily via reaction with OH.



4 Rate constants (k) are taken from the IUPAC database (Atkinson et al., 2006). These reactions
5 form the basis for a photochemical clock of isoprene oxidation (de Gouw et al., 2005; Roberts
6 et al., 2006; Stroud et al., 2001). Integration of the kinetic equations for this system shows
7 that the product/parent ratios are a function of the rate constants, yield (y), reaction time (t)
8 and mean OH concentration. In the case of MACR, for example:

9
$$\frac{[MACR]}{[ISOP]} = \frac{y_{MACR}k_1}{k_2 - k_1} (1 - \exp((k_1 - k_2)[OH]t))$$
 (1)

10 An analogous expression holds for MVK. As noted by Stroud et al. (2001), this “sequential
11 reaction model” is purely chemical and does not account for the effects of mixing and
12 transport. Indeed, this analysis relates daughter/parent ratios to an “average” photochemical
13 age, when in fact there is a broad distribution of ages in any mixed air mass. We also
14 implicitly assume that direct emissions (Fares et al., 2015) and deposition (Karl et al., 2010)
15 of MVK and MACR do not significantly influence the budget of these compounds.

16 Two potential issues arise when applying this model to the real atmosphere. First, the
17 yields of MVK and MACR are dependent on ISOPO₂ branching and are thus a non-linear
18 function of NO_x. Previous applications of this method (de Gouw et al., 2005; Roberts et al.,
19 2006; Stroud et al., 2001) have assumed lab-derived high-NO_x yields of 0.33 and 0.23 for
20 MVK and MACR, respectively (Atkinson and Arey, 2003), but this may not be appropriate in
21 the present case; furthermore, these yields are not fully consistent with current chemical
22 mechanisms (~~Fig. S4). We explicitly examine the effects of NO_x-varying yields below using~~
23 ~~yield curves derived from box model simulations (see SI for details).~~ Given the wide range of
24 conditions sampled, we explicitly account for NO_x-dependent yields for MVK and MACR.
25 For this purpose, we conducted a series of pseudo-chamber simulations using a box model
26 driven by the Master Chemical Mechanism (MCM) v3.3.1 (Jenkin et al., 2015). As described
27 in the SI, model setup mimics typical daytime conditions in the Southeast U.S. (Fig. S3B),
28 and yields are derived using a standard procedure. Resulting yield curves (Fig. S3A) are then
29 interpolated to observed NO mixing ratios. Second, the photochemical age (t) implied by any
30 observed daughter/parent ratio depends on the concentration of OH, which was not measured

1 and varies as an air mass ages. Rather than assume a single “typical” value for OH, we
2 express photochemical age in terms of “exposure,” defined here as the product of OH
3 concentration and reaction time averaged over the photochemical lifetime of an air mass.

4 Figure 2 compares the observed relationship of iWAS MVK/isoprene and
5 MACR/isoprene ratios against theoretical trends predicted by the sequential reaction model.
6 Theoretical ratios are calculated at fixed exposures of 2, 4, 8, 12 and 16×10^6 OH cm^{-3} h
7 using ~~two sets of model derived yields: high for the 5th/95th percentiles of the observed NO~~
8 ~~distribution~~ (NO = ~~100020/200~~ pptv, $y_{\text{MVK}} = 0.4118/0.38$, $y_{\text{MACR}} = 0.28$) and low NO (NO =
9 ~~50~~ pptv, $y_{\text{MVK}} = 0.21$, $y_{\text{MACR}} = 11/0.1920$). Observed ratios of MVK/isoprene versus
10 MACR/isoprene exhibit a tight linear correlation. Higher ratios are often associated with
11 higher NO_x, likely reflecting enhanced OH and higher product yields in these air masses. Far
12 downwind from isoprene and NO_x source regions, we would expect to see higher
13 MVK/isoprene and MACR/isoprene ratios associated with lower NO_x due to removal of the
14 latter. The theoretical slope agrees well with observations, indicating exposures of 1 – 16 ×
15 10^6 OH cm^{-3} h. For a typical daytime OH concentration of 4×10^6 cm^{-3} , this corresponds to
16 processing times of 0.25 – 4 hours.

17 ~~The ratio of y_{MVK} to y_{MACR} dictates the location of the theoretical line and thus~~
18 ~~assumed MVK and MACR yields dictate~~ the correspondence between daughter/parent ratios
19 and exposure. For example, a MACR/isoprene ratio of 1 would be consistent with an
20 exposure of 47.9×10^6 OH cm^{-3} h at ~~high-NO_x conditions~~ (NO = ~~100020~~ pptv) versus $6.40 \times$
21 10^6 OH cm^{-3} h at ~~low-NO_x~~ (NO = ~~50200~~ pptv). Thus, for any given daughter/parent ratio, a
22 higher assumed yield gives a smaller derived exposure. ~~Observations in Fig. 2 fall above the~~
23 ~~high-NO_x theoretical relationship. As discussed in the SI, however, iWAS MVK measurement~~
24 ~~may contain a positive artifact on the order of 34–51%. This potential systematic error (thick~~
25 ~~black line in Fig. 2) overlaps both the high and low-NO_x theoretical relationships. Given the~~
26 ~~wide range of conditions sampled, we elect to use a NO_x-dependent yield for MVK and~~
27 ~~MACR. For this purpose, model-derived yields (Fig. S4 and SI) are interpolated to observed~~
28 ~~NO mixing ratios. The ratio of y_{MVK} to y_{MACR} determines the location of the theoretical line,~~
29 ~~and the excellent agreement of this relationship with observations in Fig. 2 indicates that~~
30 ~~MCMv3.3.1 accurately represents the branching ratios for MVK and MACR production~~
31 ~~within the sampled NO_x range.~~

1 We can effectively reverse this photochemical clock to derive a proxy for the total
2 isoprene emissions that ~~had~~have been released into the sample air masses (de Gouw et al.,
3 2005). First, we calculate OH exposures from observed daughter/parent ratios by inverting
4 EqEqn. (1). To perform this calculation with PTR-MS data (which has far greater coverage
5 than the iWAS), we partition the measured sum between MVK and MACR using
6 MVK/MACR ratios from steady-state box model calculations (Sect. 5). Modeled
7 MVK/MACR ratios (with an output interval of 1 minute) are linearly interpolated to the 14-
8 second observational time base. The MVK/MACR ratio does not vary dramatically (mean \pm
9 1σ : ~~+2.3~~ ± 0.2), and using a constant ratio instead alters ~~result~~exposures by less than 4%.
10 Calculated exposures range from ~~0.51~~ to ~~+820~~ $\times 10^6$ OH cm⁻³ h (Fig. ~~S5A~~S4A). Exposures
11 derived from MACR are 6% ~~higher~~lower than those from MVK on average, and we use the
12 mean of these two values. Next, an “initial” isoprene mixing ratio, *ISOP*₀, is estimated via
13 reverse integration of isoprene’s first-order loss rate:

$$14 \quad [ISOP]_0 = [ISOP] \exp(k_1 [OH] t) \quad (2)$$

15 *ISOP*₀ represents the amount of isoprene that an air parcel would have to start with to generate
16 the amount of isoprene, MVK and MACR observed. Thus, it is an observationally-
17 constrained surrogate for isoprene emission strength (modulated to some degree by boundary
18 layer height, as it is a volume-based quantity). *ISOP*₀ mixing ratios are typically 2 – ~~+020~~
19 times higher than observed isoprene (Fig. ~~S5B~~S4B).

20

21 **4 The Yield of HCHO from Isoprene**

22 The definition of “yield” can vary with context and requires careful consideration when
23 quantifying ~~the~~chemical relationships. In a mechanistic sense, the “first generation yield”
24 refers to the amount of HCHO produced per unit isoprene consumed in the first stage of
25 oxidation. This is analogous to the yields of MVK and MACR used in the above calculation
26 of initial isoprene. The model-derived first-generation HCHO yield from isoprene varies by
27 more than a factor of 2 over the range of chemical environments encountered during SENEX
28 (Fig. ~~S4S3~~). An alternative definition is that of the “total yield” (sometimes referred to as the
29 “molar yield,” e.g. Millet et al. (2006)), a time-dependent quantity that describes the total
30 amount of HCHO produced over multiple generations of oxidation. The total yield is typically
31 derived from model simulations and used to relate satellite HCHO column observations to

1 isoprene emissions (Marais et al., 2012; Millet et al., 2006). Early studies acknowledged the
2 NO_x dependence of the total yield (Millet et al., 2006; Palmer et al., 2003), and more recent
3 work has attempted to account for this dependence using NO₂ column observations (Marais et
4 al., 2012). Here, we define the “prompt yield” as the change in observed HCHO per unit
5 change in ISOP₀ ($y_p = \Delta(\text{HCHO})/\Delta(\text{ISOP}_0)$). This is not the same as the first-generation yield,
6 since y_p the prompt yield can include HCHO production and loss over several hours
7 (depending on the photochemical exposure of an air mass). Nor is it the same as the total
8 yield, which inherently does not account for HCHO loss as an air mass ages. The prompt
9 yield is effectively a quantity that relates isoprene emission strength to observed HCHO
10 abundance. As we will demonstrate, y_p this quantity is well-suited for segregating the various
11 drivers of HCHO and for benchmarking model performance.

12 Figure 3A shows the relationship between calculated ISOP₀ and observed HCHO. The
13 overall correlation is linear with a striking NO_x gradient. To quantify this NO_x dependence,
14 we sort the data by log(NO_x), group it into 20 bins such that each bin contains the same
15 number of points (N = 416), and perform a major-axis linear fit of HCHO versus ISOP₀ for
16 each bin. Individual fits give r² values of 0.6-0.8, except for the highest NO_x bin (r² = 0.48)
17 that contains some heavily-polluted air masses, such as downwind from power plants. Very
18 fresh power plant plumes, defined as log(NO_x) values exceeding a mean + 3σ threshold, are
19 removed prior to this procedure to avoid skewing the highest NO_x bin. Results are
20 independent of the number of bins chosen or time resolution (e.g., 1-second versus 1-minute
21 data).

22 The HCHO-ISOP₀ slope (Fig. 3B) represents the prompt yield. This yield varies by a
23 factor of 3 over the range of observed NO_x, from 0.3 ppbv ppbv⁻¹ for NO_x mixing ratios of a
24 few hundred pptv to 0.9 ppbv ppbv⁻¹ at NO_x > 1 ppbv. At low NO_x, y_p the prompt yield is
25 comparable to the MCM-predicted direct first-generation yield of HCHO (0.325-0.4 ppbv
26 ppbv⁻¹ at NO = 10-40 pptv, Fig. S4S3), while at high NO_x it is somewhat higher than the
27 predicted first-generation yield (0.7475 ppbv ppbv⁻¹ at NO = 1000 pptv). This likely reflects
28 the inclusion of more than one generation of HCHO production at higher NO_x, where
29 oxidation is more rapid (median exposures increase by 38% over the range of observed NO_x
30 values). Most of this portion of the HCHO budget, however, stems from first-generation
31 production.

1 The intercept (Fig. 3C) represents the abundance of “background” HCHO. This
2 portion of the HCHO budget stems mainly from air that either has not encountered strong
3 isoprene emissions or is so aged that most of the isoprene has reacted away and can no longer
4 be linked to a specific source region. Some of this background may also stem from oxidation
5 of long-lived primary emissions like methane or methanol. Box model calculations (Sect. 5)
6 indicate average HCHO budget contributions of 0.3 ± 0.2 ppbv and 0.2 ± 0.1 ppbv from
7 methane and methanol, respectively. Background HCHO also exhibits a marked NO_x
8 dependence, increasing from 1.6 to 3.3 ppbv over the observed NO_x range. As with ~~y_p~~
9 ~~the~~ prompt yield, we expect such behavior since NO_x regulates the fate of all organic peroxy
10 radicals (see Sect. 6). Assuming a 1 km mixed layer depth (Wagner et al., 2015), the
11 corresponding HCHO column density for this background is $4 - 8 \times 10^{15} \text{ cm}^{-2}$. This is
12 comparable to the background reported by previous investigations of satellite-derived HCHO
13 columns (Barkley et al., 2013; Millet et al., 2006). None of these studies explicitly account for
14 the NO_x dependence of the background, though it can represent a substantial fraction of the
15 total HCHO column – maximum summertime HCHO columns over the southeast U.S. are
16 $\sim 25 \times 10^{15} \text{ cm}^{-2}$ (Millet et al., 2008). Given the strong NO_x dependence of both ~~y_p~~
17 ~~prompt~~ background HCHO, grouping HCHO column observations by NO_x (e.g. using simultaneous
18 observations of NO_2 columns (Marais et al., 2012) or model-derived NO_x) and performing an
19 analysis similar to that described here ~~should~~could provide a robust means of accounting for
20 these influences.

21

22 5 Model Evaluation

23 Next, we compare the observed HCHO-ISOP₀ relationship to results from a global chemical-
24 transport model and a 0-D box model. Our goals are to both illustrate the utility of this
25 analysis and evaluate model performance. By going beyond a simple comparison of modeled
26 and measured mixing ratios, we can more accurately pinpoint potential shortcomings in
27 model chemistry.

28 The GFDL AM3 model is an atmospheric general circulation model with interactive
29 chemistry (Donner et al., 2011), including recent updates to the representation of isoprene
30 degradation (Mao et al., 2013; Naik et al., 2013). Model simulations were carried out at $50 \times$
31 50 km^2 resolution with horizontal winds nudged to NCEP GFS analyses and sampled along

1 the SENEX flight tracks at a time resolution of 1 minute. Further details are available
2 elsewhere (~~Li et al., 2015~~)([Li et al., 2016](#)).

3 The University of Washington Chemical Box Model (UWCM v2.2) is a versatile 0-
4 dimensional framework for simulating various chemical systems, including lab chamber
5 experiments (Wolfe et al., 2012) and observations from ground (Kim et al., 2015; Kim et al.,
6 2013; Wolfe et al., 2014) and airborne (Marvin et al., 2015) platforms. Multiple chemical
7 mechanisms are available within UWCM; here we used the latest version of the Master
8 Chemical Mechanism (MCM v3.3.1, ~~Jenkin et al. (2015)~~[Jenkin et al. \(2015\)](#)). UWCM was
9 constrained with 1-minute average observations of isoprene, NO₂, ozone, CO, PAN, methane,
10 methanol and meteorology and assumed clear-sky conditions for photolysis frequencies. The
11 chemical system was integrated forward in time to diel steady state (total integration time of 3
12 days) for each set of measurements. This setup inherently assumes that the atmosphere is in
13 chemical steady state – that is, that production and loss of HCHO, MVK, MACR and other
14 species are roughly balanced. This assumption is rarely strictly true and may fail for highly-
15 aged air masses (where isoprene is depleted) or when close to strong local emissions.
16 Nonetheless, it is a fair approximation for the daytime well-mixed boundary layer
17 observations that prevailed during SENEX. Monoterpenes and anthropogenic VOC are
18 excluded from the simulation since observations of these species (from the iWAS) are
19 relatively sparse. Separate sensitivity simulations utilizing the iWAS data suggest that
20 observed monoterpenes and anthropogenic VOC (a subset of alkanes, alkenes and aromatics)
21 increase modeled HCHO by $1 \pm 2\%$ and $2 \pm 3\%$, respectively. A more detailed evaluation of
22 box model performance is forthcoming (Marvin et al., 2015).

23 Output from both models is filtered for daytime, boundary-layer, non-biomass burning
24 points using the same criteria as that for observations (Sect. 2). Both models adequately
25 reproduce observed HCHO mixing ratios (Fig. ~~S6S5~~). We perform the same analyses as
26 described above to derive model y_p prompt yield and background HCHO. Because of the
27 reduced time resolution, we group results into 10 NO_x bins, instead of 20, before fitting. For
28 AM3, this results in 172 points per bin and typical r^2 values of 0.54 – 0.8. For UWCM, there
29 are ~~157134~~ points per bin and all r^2 values are > 0.986 .

30 Both AM3 and UWCM reproduce the observed NO_x dependence of the prompt yield
31 (Fig. 4A). AM3 agrees well with observations in both magnitude and trend, though with some
32 scatter at mid-NO_x levels. UWCM tends to be slightly highlow throughout most of the whole

1 NO_x range, which may reflect an ~~over-estimation of first-generation HCHO production due to~~
2 ~~holding isoprene constant throughout~~ ~~the model step and/mechanism (discussed~~
3 ~~below) or assuming a~~ ~~inherent shortcoming of the~~ steady-state ~~assumption~~. Regardless
4 ~~of minor differences~~, these results suggest that both models provide excellent representation
5 of early generation isoprene oxidation across NO_x regimes—~~despite using dramatically~~
6 ~~different chemical mechanisms~~.

7 Background HCHO mixing ratios are under-predicted by 0.5 – 1 ppbv by both models
8 (Fig. 4B). The range of under-prediction is consistent with the offsets between observed and
9 modeled total HCHO abundances (Fig. S6S5 fit x-intercepts: 0.3 ppbv (AM3) and ~~0.91.1~~
10 ppbv (UWCM)). It is possible that both models are missing some HCHO precursors (e.g.
11 from multi-generation isoprene oxidation or other VOC not related to isoprene). This is
12 especially plausible for the UWCM simulation, which only includes isoprene, methane and
13 methanol as primary VOC and does not account for horizontal transport. Under-estimated OH
14 concentrations might also explain part of this discrepancy, though we cannot easily evaluate
15 this possibility. AM3 performs somewhat better than UWCM in terms of overall magnitude
16 but exhibits a less clear NO_x trend, which may reflect dilution over fairly large grid scales
17 (note that the range of binned NO_x values is smaller for AM3 than both observations and the
18 UWCM). This result again highlights the need to consider this background before using a
19 model to interpret observed HCHO columns that effectively ~~integrate average~~ HCHO sources
20 over space and time.

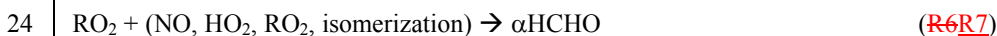
21 ~~The agreement between AM3 and UWCM-MCMv3.3.1 is consistent with how these~~
22 ~~mechanisms treat first-generation ISOPO₂ radicals (Figs. S6 and S7). Both models use the~~
23 ~~same rate constants for reactions of ISOPO₂ with NO and HO₂, which comprise the bulk of~~
24 ~~ISOPO₂ sink. The AM3 mechanism assigns a 12% yield of HCHO to the reaction of ISOPO₂~~
25 ~~with HO₂ (Paulot et al., 2009b), while the MCM assumes 100% production of peroxides for~~
26 ~~this channel. This may explain some of the discrepancy in the prompt yield at low NO_x (Fig.~~
27 ~~4A), though neither mechanism is consistent with the current experimental HCHO yield of~~
28 ~~~6% HCHO (Liu et al., 2013). There are also two key differences in the minor reaction~~
29 ~~channels. First, the rate constant for reaction of ISOPO₂ with other RO₂ is an order of~~
30 ~~magnitude lower in AM3 compared to MCMv3.3.1 (1.54 vs. $12 - 16 \times 10^{-13} \text{ cm}^3 \text{ s}^{-1}$, the latter~~
31 ~~depending on the ISOPO₂ isomer distribution). This reaction produces HCHO with yields~~
32 ~~comparable to that of ISOPO₂ + NO and may be an important source in very-low NO_x~~

1 regimes. Second, AM3 assumes a constant ISOPO₂ isomer distribution and thus under-
2 predicts the isomerization rate relative to MCMv3.3.1, especially at mid to high NO_x (Fig.
3 S7D). AM3 also includes HCHO and other small oxidized VOC as direct products of
4 isomerization rather than producing hydroperoxyaldehydes and other large products, which
5 influences the timescale of HCHO production and thus the partitioning between prompt and
6 background HCHO. The impact of the RO₂ reaction and isomerization channels on HCHO
7 yields is likely minor but depends significantly on the RO₂/HO₂ ratio (at low NO_x) and on the
8 overall ISOPO₂ lifetime, which affects the ISOPO₂ isomer distribution. For the particular
9 model conditions in Fig. S3B, ISOPO₂ lifetimes for the two mechanisms can differ by as
10 much as 25% at the lowest NO_x values (Fig. S7E). Regardless of these differences, the results
11 shown in Fig. 4 confirm that both the condensed AM3 and explicit MCMv3.3.1 mechanisms
12 perform similarly with regard to overall HCHO production.

13

14 **6 Mechanistic Drivers of the NO_x – HCHO Relationship**

15 Despite the complexity of gas-phase organic chemistry, the impact of NO_x on HCHO
16 production essentially reduces to two factors: radical cycling and RO₂ branching. Increasing
17 NO enhances the conversion of HO₂ to OH (R4) and thus accelerates VOC oxidation (R5)
18 ~~and HCHO loss~~. RO₂ is also produced, to a lesser extent, by VOC ozonolysis and photolysis
19 (R6). Subsequent production of HCHO depends on the structure and fate of RO₂
20 intermediates, which can react with NO, HO₂, other RO₂, or isomerize (~~R6~~R7).



25 Here, α represents a bulk branching ratio for HCHO production weighted over all RO₂
26 reactions. The RO₂ lifetime is typically less than 100 s during the day, so (R5) is the rate-
27 limiting step in HCHO formation. The HCHO production rate is then equal to the product of
28 the total RO₂ production rate and the bulk branching ratio:

29 $P(\text{HCHO}) = \alpha P(\text{RO}_2) \quad (3)$

1 Though total RO₂ losses include reactions that do not make HCHO, α is still a useful metric
2 for the relationship between HCHO production and overall VOC oxidation.

3 To disentangle these factors, we extract chemical rates from the diel steady-state
4 UWCM simulations discussed in Sect. 5. Figure 55A shows the gross production rates for
5 total peroxy radicals and HCHO as a function of NO_x. Consistent with our earlier discussion,
6 ~~total~~ HCHO production increases by ~~more than~~ a factor of 3 from low to high NO_x. ~~In~~
7 ~~contrast,~~ Total RO₂ production is effectively constant within model variability. Closer scrutiny
8 reveals that a increases by a factor of 3—4 increase in 2 over this same range, driven
9 primarily by increasing OH concentrations between low and high NO_x is more than offset by
10 a concomitant reduction in isoprene (results not shown). The bulk branching ratio α ,
11 calculated as the ratio of HCHO to and RO₂ production rates gives an estimate for α , which,
12 increases from 0.14 to 0.39 across this NO_x range (Fig. 5). Though the total RO₂ production
13 rate includes reactions that do not make HCHO, α is still a useful metric for the relationship
14 between HCHO production 43 to 0.62 (Fig. 5B). This trend is consistent with NO_x-dependent
15 branching ratios of several major HCHO precursors, including isoprene hydroxyperoxy
16 radicals (ISOPO₂) and overall VOC oxidation, methyl peroxy radical (Fig. 5B). Based on this
17 analysis, we conclude that ~~changes in RO₂ branching are the dominant factor driving~~
18 enhanced OH production is the main driver for the NO_x dependence of HCHO production and
19 abundance, with variations in RO₂ branching playing a lesser (but still important) role.

20 Using a combination of regional modeling and satellite observations, a recent study by
21 Valin et al. (2016) also examines the drivers of HCHO production. They concur that OH
22 production exerts a controlling influence on HCHO throughout the Southeast U.S. In contrast
23 to our study, however, they assert that changes in RO₂ branching have a negligible effect on
24 the HCHO-NO_x dependence. There are several potential explanations for this discrepancy.
25 First, Valin et al. (2016) derive an “effective branching ratio” that is analogous to the bulk
26 branching ratio in Eqn. (3) but calculated with reference to production of OH rather than RO₂.
27 Many OH sinks do not form RO₂ radicals (e.g. reaction with CO, HCHO, methanol and NO₂)
28 and thus will not make HCHO. The fractional contribution of such reactants to total modeled
29 OH reactivity increases from 36% to 60% over our NO_x range; thus, using P(OH) instead of
30 P(RO₂) to calculate α from Eqn. (3) would effectively normalize out the NO_x dependence of
31 RO₂ branching (Fig. 5B). Second, these two studies use very different photochemical
32 mechanisms. Valin et al. (2016) use a modified version of the lumped Regional Atmospheric

Formatted: Not Superscript/ Subscript

1 Chemistry Mechanism 2 (RACM2) (Browne et al., 2014; Goliff et al., 2013), while our box
2 model uses the explicit MCMv3.3.1 (Jenkin et al., 2015). In Valin et al. (2016), it is stated
3 that decreasing HCHO production from the RO₂ + NO channel is compensated for by
4 increasing production from RO₂ + RO₂ – an effect that we do not observe. Deeper
5 investigation reveals that the rate constant for reaction of ISOPO₂ with HO₂ in RACM2,
6 which is based on work by Paulot et al. (2009b), is a factor of 2 lower than those used in both
7 MCMv3.3.1 and the AM3 mechanism. Thus, our model predicts a significantly larger
8 contribution of RO₂ + HO₂ (which produces negligible HCHO) to the total RO₂ sink. These
9 differences highlight the importance of carefully evaluating chemical mechanisms before
10 using models to interpret *in situ* and satellite observations.

11 Increased OH also reduces the lifetime of HCHO, which may affect the HCHO budget
12 if this reaction becomes competitive with photolysis. UWCM predicts an average HCHO
13 photolysis lifetime of 4 hours and OH reaction lifetimes that range from 3 hours at high NO_x
14 to 12 hours at low NO_x. Thus, photolysis is typically the dominant loss process and the
15 scaling of HCHO lifetime with OH is typically weak. ~~As a result, the~~The net chemical
16 tendency of HCHO (production minus loss) is positive and increasing throughout the range of
17 model NO_x conditions. Faster loss due to reaction with OH therefore only slightly dampens
18 the enhancement in HCHO production.

19

20 **7 Conclusions**

21 Using SENEX aircraft observations, we have quantified the NO_x dependence of the
22 relationship between isoprene emission strength and HCHO mixing ratios. Simultaneous
23 measurements of isoprene, MVK and MACR define a photochemical clock for isoprene
24 oxidation, allowing separation of prompt HCHO production (which retains the isoprene
25 source signature) and background HCHO from late-generation isoprene oxidation products,
26 methane and other long-lived VOC. The prompt HCHO yield increases by a factor of 3 (0.3 to
27 0.9 ppbv ppbv⁻¹) and the average background HCHO mixing ratio ~~more than~~doubles (1.6 to
28 3.3 ppbv) over the range of NO_x values encountered in the southeast U.S. (0.1 – 2 ppbv). This
29 analytical method is applied to evaluate the performance of a global chemical transport model
30 and a 0-D steady-state box model. Both models accurately reproduce the observed NO_x trend
31 of the prompt HCHO yield, indicating that both chemical mechanisms accurately capture
32 early-stage isoprene oxidation. On the other hand, both models also under-predict background

1 HCHO abundance by 0.5 – 1 ppbv, which ~~can be~~ is a significant fraction of total HCHO in
2 some cases. This ~~may suggest~~ suggests insufficient build-up of isoprene-derived long-lived
3 precursors in the models, missing VOC not related to isoprene, or insufficient OH. Box model
4 results also provide insight into the mechanistic drivers of the observed NO_x trends. ~~We find~~
5 ~~that increasing~~ Over the NO_x ~~does not significantly affect~~ range studied here, a 100% increase
6 ~~in~~ total RO₂ production ~~due to the cancelling effects of higher OH and lower VOC. Thus, a~~
7 ~~40% increase in~~ the ~~positive correlation between NO_x and HCHO~~ primarily reflects the
8 ~~changing fate of RO₂ radicals~~ production branching ratio give rise to a 3-fold increase in total
9 HCHO production.

10 To our knowledge, there are no direct laboratory measurements of HCHO yields from
11 low-NO_x isoprene chemistry; thus, the results presented here constitute the first measurement-
12 constrained evaluation of the isoprene-HCHO link across NO_x regimes. The AM3 and
13 MCMv3.3.1 mechanisms differ substantially (the former is highly condensed while the latter
14 is explicit), but both contain recent updates to isoprene degradation. We expect that other
15 mechanisms will also perform well if they accurately reflect our current best understanding.
16 The observations presented here do not include the extremely-low NO_x regime (NO_x < 0.1
17 ppbv) typical of remote regions like the Amazon and equatorial Africa. In such pristine
18 regions, smearing of HCHO production is expected to be more severe (Barkley et al., 2013),
19 and total HCHO production may be significantly lower if the RO₂ fate favors
20 functionalization over fragmentation (e.g. isomerization). More work is needed to map out
21 this area of the urban-rural spectrum. It may also be possible to apply the methods developed
22 here to evaluate the chemistry of glyoxal, another key tracer of VOC oxidation that is also
23 amenable to orbital observations (~~Kaiser et al., 2015b; Li et al., 2015~~)(Kaiser et al., 2015b; Li
24 et al., 2016) and is believed to be an important precursor for SOA (McNeill et al., 2012).

25 These results also carry implications for top-down isoprene emission estimates.
26 Uncertainties in low-NO_x chemistry are often cited as the largest source of potential error in
27 derived emissions (Marais et al., 2012; Palmer et al., 2006). Based on our analysis, current
28 mechanisms appear to capture low-NO_x production of HCHO, MVK and MACR, thus such
29 errors are likely less severe than commonly asserted. Recent work has acknowledged the
30 impact of NO_x on the prompt yield of HCHO from isoprene (Marais et al., 2012). We
31 advocate considering the NO_x dependence of background HCHO as well, since this can
32 constitute a significant fraction of the total HCHO column. For scale, the derived background

1 HCHO mixing ratio of 1.6 – 3.3 ppbv is 37 – 77% of the campaign-mean observed HCHO
2 mixing ratio of 4.3 ppbv. Forthcoming geostationary observations will resolve local gradients
3 in chemical regime, and smearing and background HCHO production will become
4 problematic even in high-NO_x regions. Indeed, even current-generation orbital instruments are
5 capable of resolving some urban-rural gradients in HCHO columns (Boeke et al., 2011).
6 When applying advanced statistical techniques like inversion, model results will only be as
7 accurate as the chemical mechanisms driving them. Continued field observations are crucial
8 for providing confidence in our ability to link HCHO to its sources. In this regard, recent
9 work has highlighted the potential of airborne eddy covariance fluxes to quantify both
10 surface-atmosphere exchange and *in situ* chemical processes (Karl et al., 2013; Kaser et al.,
11 2015; Misztal et al., 2014; Wolfe et al., 2015). With such tools, it should be possible to
12 simultaneously measure both isoprene emissions and HCHO columns, thereby obtaining a
13 direct experimental constraint on the link between these two quantities.

14

15 **Data Availability**

16 All data used in this study are publicly accessible on the SENEX website
17 (<http://www.esrl.noaa.gov/csd/projects/senex/>).

18

19 **Acknowledgements**

20 We are grateful to NOAA AOC and the flight crew of the WP-3D for enabling a super
21 awesome mission. HCHO measurement efforts were supported by US EPA Science to
22 Achieve Results (STAR) program grant 83540601 and NASA grant NNH10ZDA001N-
23 SEAC4RS. Analysis was supported by NASA ACCDAM grant NNX14AP48G. J. Kaiser
24 acknowledges support from NASA ESSF grant NNX14AK97H. C.D. Hatch was supported by
25 the Hendrix faculty grant and the Hendrix College Odyssey program. JM and LWH
26 acknowledge support from NOAA Climate Program Office grant # NA13OAR4310071. This
27 research has not been subjected to any EPA review and therefore does not necessarily reflect
28 the views of the agency, and no official endorsement should be inferred.

29

1 **References**

- 2 Abbot, D. S., Palmer, P. I., Martin, R. V., Chance, K. V., Jacob, D. J., and Guenther, A.:
3 Seasonal and interannual variability of North American isoprene emissions as determined by
4 formaldehyde column measurements from space, *Geophys. Res. Lett.*, 30, 1886, doi:
5 10.1029/2003GL017336, 2003.
- 6 Atkinson, R. and Arey, J.: Gas-phase tropospheric chemistry of biogenic volatile organic
7 compounds: a review, *Atmos. Env.*, 37, S197 - S219, 2003.
- 8 Atkinson, R., Baulch, D., Cox, R., Crowley, J., Hampson, R., Hynes, R., Jenkin, M., Rossi,
9 M., and Troe, J.: Evaluated kinetic and photochemical data for atmospheric chemistry:
10 Volume II - gas phase reactions of organic species, *Atmos. Chem. Phys.*, 6, 3625-4055, 2006.
- 11 Barkley, M. P., De Smedt, I., Van Roozendaal, M., Kurosu, T. P., Chance, K., Arneeth, A.,
12 Hagberg, D., Guenther, A., Paulot, F., Marais, E., and Mao, J. Q.: Top-down isoprene
13 emissions over tropical South America inferred from SCIAMACHY and OMI formaldehyde
14 columns, *J. Geophys. Res. Atmos.*, 118, 6849-6868, doi: 10.1002/jgrd.50552, 2013.
- 15 Barkley, M. P., Palmer, P. I., Kuhn, U., Kesselmeier, J., Chance, K., Kurosu, T. P., Martin, R.
16 V., Helmig, D., and Guenther, A.: Net ecosystem fluxes of isoprene over tropical South
17 America inferred from Global Ozone Monitoring Experiment (GOME) observations of
18 HCHO columns, *J. Geophys. Res.*, 113, D20304, doi: 10.1029/2008JD009863, 2008.
- 19 Boeke, N. L., Marshall, J. D., Alvarez, S., Chance, K. V., Fried, A., Kurosu, T. P.,
20 Rappengluck, B., Richter, D., Walega, J., Weibring, P., and Millet, D. B.: Formaldehyde
21 columns from the Ozone Monitoring Instrument: Urban versus background levels and
22 evaluation using aircraft data and a global model, *J. Geophys. Res. Atmos.*, 116, D05303, doi:
23 10.1029/2010jd014870, 2011.
- 24 [Brown, S. S., deGouw, J. A., Warneke, C., Ryerson, T. B., Dube, W. P., Atlas, E., Weber, R.](#)
25 [J., Peltier, R. E., Neuman, J. A., Roberts, J. M., Swanson, A., Flocke, F., McKeen, S. A.,](#)
26 [Brioude, J., Sommariva, R., Trainer, M., Fehsenfeld, F. C., and Ravishankara, A. R.:](#)
27 [Nocturnal isoprene oxidation over the Northeast United States in summer and its impact on](#)
28 [reactive nitrogen partitioning and secondary organic aerosol, *Atmos. Chem. Phys.*, 9, 3027-](#)
29 [3042, 2009.](#)

1 [Browne, E. C., Wooldridge, P. J., Min, K. E., and Cohen, R. C.: On the role of monoterpene](#)
2 [chemistry in the remote continental boundary layer, *Atmos. Chem. Phys.*, 14, 1225-1238, doi:](#)
3 [10.5194/acp-14-1225-2014, 2014.](#)

4 Carlton, A. and Baker, K.: Photochemical Modeling of the Ozark Isoprene Volcano:
5 MEGAN, BEIS, and Their Impacts on Air Quality Predictions, *Env. Sci. Technol.*, 45, 4438-
6 4445, doi: 10.1021/es200050x, 2011.

7 Cazorla, M., Wolfe, G. M., Bailey, S. A., Swanson, A. K., Arkinson, H. L., and Hanisco, T.
8 F.: A new airborne laser-induced fluorescence instrument for in situ detection of
9 Formaldehyde throughout the troposphere and lower stratosphere, *Atmos. Meas. Tech.*, 8,
10 541-552, doi: 10.5194/amt-8-541-2015, 2015.

11 Crounse, J. D., Knap, H. C., Ørnsø, K. B., Jørgensen, S., Paulot, F., Kjaergaard, H. G., and
12 Wennberg, P. O.: On the atmospheric fate of methacrolein: 1. Peroxy radical isomerization
13 following addition of OH and O₂, *J. Phys. Chem. A*, 116, 5756-5762, doi:
14 10.1021/jp211560u, 2012.

15 Crounse, J. D., Paulot, F., Kjaergaard, H. G., and Wennberg, P. O.: Peroxy radical
16 isomerization in the oxidation of isoprene, *Phys. Chem. Chem. Phys.*, 13, 13607-13613, 2011.

17 Curci, G., Palmer, P. I., Kurosu, T. P., Chance, K., and Visconti, G.: Estimating European
18 volatile organic compound emissions using satellite observations of formaldehyde from the
19 Ozone Monitoring Instrument, *Atmos. Chem. Phys.*, 10, 11501-11517, doi: 10.5194/acp-10-
20 11501-2010, 2010.

21 da Silva, G., Graham, C., and Wang, Z. F.: Unimolecular beta-Hydroxyperoxy Radical
22 Decomposition with OH Recycling in the Photochemical Oxidation of Isoprene, *Env. Sci.*
23 *Technol.*, 44, 250-256, 2010.

24 de Gouw, J. and Warneke, C.: Measurements of volatile organic compounds in the earths
25 atmosphere using proton-transfer-reaction mass spectrometry, *Mass Spec. Rev.*, 26, 223-257,
26 doi: 10.1002/mas.20119, 2007.

27 de Gouw, J. A., McKeen, S. A., Aikin, K. C., Brock, C. A., Brown, S. S., Gilman, J. B.,
28 Graus, M., Hanisco, T., Holloway, J. S., Kaiser, J., Keutsch, F. N., Lerner, B. M., Liao, J.,

1 Markovic, M. Z., Middlebrook, A. M., Min, K. E., Neuman, J. A., Nowak, J. B., Peischl, J.,
2 Pollack, I. B., Roberts, J. M., Ryerson, T. B., Trainer, M., Veres, P. R., Warneke, C., Welti,
3 A., and Wolfe, G. M.: Airborne Measurements of the Atmospheric Emissions from a Fuel
4 Ethanol Refinery, *J. Geophys. Res. Atmos.*, 120, 4385-4397, doi: 10.1002/2015jd023138,
5 2015.

6 de Gouw, J. A., Middlebrook, A. M., Warneke, C., Goldan, P. D., Kuster, W. C., Roberts, J.
7 M., Fehsenfeld, F. C., Worsnop, D. R., Canagaratna, M. R., Pszenny, A. A. P., Keene, W. C.,
8 Marchewka, M., Bertman, S. B., and Bates, T. S.: Budget of organic carbon in a polluted
9 atmosphere: Results from the New England Air Quality Study in 2002, *J. Geophys. Res.*, 110,
10 D16305, doi: 10.1029/2004jd005623, 2005.

11 DiGangi, J. P., Boyle, E. S., Karl, T., Harley, P., Turnipseed, A., Kim, S., Cantrell, C.,
12 Maudlin Iii, R. L., Zheng, W., Flocke, F., Hall, S. R., Ullmann, K., Nakashima, Y., Paul, J.
13 B., Wolfe, G. M., Desai, A. R., Kajii, Y., Guenther, A., and Keutsch, F. N.: First direct
14 measurements of formaldehyde flux via eddy covariance: implications for missing in-canopy
15 formaldehyde sources, *Atmos. Chem. Phys.*, 11, 10565-10578, doi: 10.5194/acp-11-10565-
16 2011, 2011.

17 Donner, L. J., Wyman, B. L., Hemler, R. S., Horowitz, L. W., Ming, Y., Zhao, M., Golaz, J.-
18 C., Ginoux, P., Lin, S. J., Schwarzkopf, M. D., Austin, J., Alaka, G., Cooke, W. F., Delworth,
19 T. L., Freidenreich, S. M., Gordon, C. T., Griffies, S. M., Held, I. M., Hurlin, W. J., Klein, S.
20 A., Knutson, T. R., Langenhorst, A. R., Lee, H.-C., Lin, Y., Magi, B. I., Malyshev, S. L.,
21 Milly, P. C. D., Naik, V., Nath, M. J., Pincus, R., Ploshay, J. J., Ramaswamy, V., Seman, C.
22 J., Shevliakova, E., Sirutis, J. J., Stern, W. F., Stouffer, R. J., Wilson, R. J., Winton, M.,
23 Wittenberg, A. T., and Zeng, F.: The Dynamical Core, Physical Parameterizations, and Basic
24 Simulation Characteristics of the Atmospheric Component AM3 of the GFDL Global
25 Coupled Model CM3, *J. Climate*, 24, 3484-3519, doi: 10.1175/2011jcli3955.1, 2011.

26 Dufour, G., Wittrock, F., Camredon, M., Beekmann, M., Richter, A., Aumont, B., and
27 Burrows, J. P.: SCIAMACHY formaldehyde observations: constraint for isoprene emission
28 estimates over Europe?, *Atmos. Chem. Phys.*, 9, 1647-1664, 2009.

1 Fares, S., Paoletti, E., Loreto, F., and Brillì, F.: Bidirectional Flux of Methyl Vinyl Ketone
2 and Methacrolein in Trees with Different Isoprenoid Emission under Realistic Ambient
3 Concentrations, *Environ Sci Technol*, 49, 7735-7742, doi: 10.1021/acs.est.5b00673, 2015.

4 Fortems-Cheiney, A., Chevallier, F., Pison, I., Bousquet, P., Saunois, M., Szopa, S., Cressot,
5 C., Kurosu, T. P., Chance, K., and Fried, A.: The formaldehyde budget as seen by a global-
6 scale multi-constraint and multi-species inversion system, *Atmos. Chem. Phys.*, 12, 6699-
7 6721, doi: 10.5194/acp-12-6699-2012, 2012.

8 Fu, T. M., Jacob, D. J., Palmer, P. I., Chance, K., Wang, Y. X. X., Barletta, B., Blake, D. R.,
9 Stanton, J. C., and Pilling, M. J.: Space-based formaldehyde measurements as constraints on
10 volatile organic compound emissions in east and south Asia and implications for ozone, *J.*
11 *Geophys. Res. Atmos.*, 112, D06312, doi: 10.1029/2006jd007853, 2007.

12 Fuchs, H., Hofzumahaus, A., Rohrer, F., Bohn, B., Brauers, T., Dorn, H., Haseler, R.,
13 Holland, F., Kaminski, M., Li, X., Lu, K., Nehr, S., Tillmann, R., Wegener, R., and Wahner,
14 A.: Experimental evidence for efficient hydroxyl radical regeneration in isoprene oxidation,
15 *Nature Geosci.*, 6, 1023-1026, doi: 10.1038/NGEO1964, 2013.

16 [Goliff, W. S., Stockwell, W. R., and Lawson, C. V.: The regional atmospheric chemistry
17 mechanism, version 2, *Atmos. Env.*, 68, 174-185, doi: 10.1016/j.atmosenv.2012.11.038,
18 2013.](#)

19 [González Abad, G., Liu, X., Chance, K., Wang, H., Kurosu, T. P., and Suleiman, R.: Updated
20 Smithsonian Astrophysical Observatory Ozone Monitoring Instrument \(SAO OMI\)
21 formaldehyde retrieval, *Atmos. Meas. Tech.*, 8, 19-32, doi: 10.5194/amt-8-19-2015, 2015.](#)

22 Guenther, A. B., Jiang, X., Heald, C. L., Sakulyanontvittaya, T., Duhl, T., Emmons, L. K.,
23 and Wang, X.: The Model of Emissions of Gases and Aerosols from Nature version 2.1
24 (MEGAN2.1): an extended and updated framework for modeling biogenic emissions, *Geosci.*
25 *Mod. Dev.*, 5, 1471-1492, doi: 10.5194/gmd-5-1471-2012, 2012.

26 Hogrefe, C., Isukapalli, S. S., Tang, X. G., Georgopoulos, P. G., He, S., Zalewsky, E. E., Hao,
27 W., Ku, J. Y., Key, T., and Sistla, G.: Impact of Biogenic Emission Uncertainties on the
28 Simulated Response of Ozone and Fine Particulate Matter to Anthropogenic Emission
29 Reductions, *J. Air Waste Man. Assoc.*, 61, 92-108, doi: 10.3155/1047-3289.61.1.92, 2011.

1 Jenkin, M. E., Young, J. C., and Rickard, A. R.: The MCM v3.3.1 degradation scheme for
2 isoprene, *Atmos. Chem. Phys. Discuss.*, 15, [9709-9766](https://doi.org/10.5194/acpd-15-9709-2015)[11433-11459](https://doi.org/10.5194/acpd-15-9709-2015), doi: 10.5194/acpd-
3 15-9709-2015, 2015.

4 Kaiser, J., Wolfe, G. M., Bohn, B., Broch, S., Fuchs, H., Ganzeveld, L. N., Gomm, S.,
5 Haseler, R., Hofzumahaus, A., Holland, F., Jager, J., Li, X., Lohse, I., Lu, K., Prevot, A. S.
6 H., Rohrer, F., Wegener, R., Wolf, R., Mentel, T. F., Kiendler-Scharr, A., Wahner, A., and
7 Keutsch, F. N.: Evidence for an unidentified non-photochemical ground-level source of
8 formaldehyde in the Po Valley with potential implications for ozone production, *Atmos.*
9 *Chem. Phys.*, 15, 1289-1298, doi: 10.5194/acp-15-1289-2015, 2015a.

10 Kaiser, J., Wolfe, G. M., Min, K. E., Brown, S. S., Miller, C. C., Jacob, D. J., deGouw, J. A.,
11 Graus, M., Hanisco, T. F., Holloway, J., Peischl, J., Pollack, I. B., Ryerson, T. B., Warneke,
12 C., Washenfelder, R. A., and Keutsch, F. N.: Reassessing the ratio of glyoxal to formaldehyde
13 as an indicator of hydrocarbon precursor speciation, *Atmos. Chem. Phys.*, 15, 7571-7583, doi:
14 10.5194/acp-15-7571-2015, 2015b.

15 Karl, T., Harley, P., Emmons, L., Thornton, B., Guenther, A., Basu, C., Turnipseed, A., and
16 Jardine, K.: Efficient Atmospheric Cleansing of Oxidized Organic Trace Gases by
17 Vegetation, *Science*, 330, 816 - 819, doi: 10.1126/science.1192534, 2010.

18 [Karl, T., Misztal, P., Jonsson, H., Shertz, S., Goldstein, A., and Guenther, A.: Airborne Flux](#)
19 [Measurements of BVOCs above Californian Oak Forests: Experimental Investigation of](#)
20 [Surface and Entrainment Fluxes, OH Densities, and Damkohler Numbers, *J. Atmos. Sci.*, 70,](#)
21 [3277-3287, doi: 10.1175/JAS-D-13-054.1, 2013.](#)

22 [Kaser, L., Karl, T., Yuan, B., Mauldin III, R. L., Cantrell, C. A., Guenther, A. B., Patton, E.](#)
23 [G., Weinheimer, A. J., Knote, C., Orlando, J., Emmons, L., Apel, E., Hornbrook, R., Shertz,](#)
24 [S., Ullmann, K., Hall, S., Graus, M., de Gouw, J., Zhou, X., and Ye, C.: Chemistry-turbulence](#)
25 [interactions and mesoscale variability influence the cleansing efficiency of the atmosphere,](#)
26 [Geophys. Res. Lett., 42, 10894-10903, doi: 10.1002/2015GL066641, 2015.](#)

27 Kefauver, S. C., Filella, I., and Peñuelas, J.: Remote sensing of atmospheric biogenic volatile
28 organic compounds (BVOCs) via satellite-based formaldehyde vertical column assessments,
29 *Int. J. Remote Sens.*, 35, 7519-7542, doi: 10.1080/01431161.2014.968690, 2014.

1 Kim, S., Kim, S. Y., Lee, M., Shim, H., Wolfe, G. M., Guenther, A. B., He, A., Hong, Y., and
2 Han, J.: Impact of isoprene and HONO chemistry on ozone and OVOC formation in a
3 semirural South Korean forest, *Atmos. Chem. Phys.*, 15, 4357-4371, doi: 10.5194/acp-15-
4 4357-2015, 2015.

5 Kim, S., Wolfe, G. M., Mauldin, L., Cantrell, C., Guenther, A., Karl, T., Turnipseed, A.,
6 Greenberg, J., Hall, S. R., Ullmann, K., Apel, E., Hornbrook, R., Kajii, Y., Nakashima, Y.,
7 Keutsch, F. N., DiGangi, J. P., Henry, S. B., Kaser, L., Schnitzhofer, R., Graus, M., Hansel,
8 A., Zheng, W., and Flocke, F. F.: Evaluation of HOx sources and cycling using measurement-
9 constrained model calculations in a 2-methyl-3-butene-2-ol (MBO) and monoterpene (MT)
10 dominated ecosystem, *Atmos. Chem. Phys.*, 13, 2031-2044, doi: 10.5194/acp-13-2031-2013,
11 2013.

12 Knighton, W. B., Herndon, S. C., Franklin, J. F., Wood, E. C., Wormhoudt, J., Brooks, W.,
13 Fortner, E. C., and Allen, D. T.: Direct measurement of volatile organic compound emissions
14 from industrial flares using real-time online techniques: Proton Transfer Reaction Mass
15 Spectrometry and Tunable Infrared Laser Differential Absorption Spectroscopy, *Industrial &*
16 *Engineering Chemistry Research*, 51, 12674-12684, doi: 10.1021/ie202695v, 2012.

17 [Kwok, E. S. C., Aschmann, S. M., Arey, J., and Atkinson, R.: Product formation from the](#)
18 [reaction of the NO₃ radical with isoprene and rate constants for the reactions of methacrolein](#)
19 [and methyl vinyl ketone with the NO₃ radical. *Int. J. Chem. Kin.*, 28, 925-934, 1996.](#)

20 Lee, M., Heikes, B. G., Jacob, D. J., Sachse, G., and Anderson, B.: Hydrogen peroxide,
21 organic hydroperoxide, and formaldehyde as primary pollutants from biomass burning, *J.*
22 *Geophys. Res. Atmos.*, 102, 1301-1309, doi: 10.1029/96jd01709, 1997.

23 Lerner, B. M., Gilman, J. B., Kuster, W. ~~C.~~, and de Gouw, J. A., et al.: An improved,
24 automated whole-air sampler and VOC GC-MS analysis system, in preparation, ~~2015~~2016.

25 Li, J., Mao, J., Min, K. E., Washenfelder, R. A., Brown, S. S., Kaiser, J., Keutsch, F. ~~NN.~~
26 [Volkamer, R.](#), Wolfe, G. M., Hanisco, T. F., Pollack, I. B., Ryerson, T. B., Graus, M.,
27 Gilman, J. B., Lerner, B. M., Warneke, C., de Gouw, J. A., ~~Broek, C. A.~~ Middlebrook, A. M.,
28 [Liao, J., Welti, A.](#), Henderson, B. H., ~~Naik, V.~~ [Donner, L. J., Cooke, W. E.](#), Paulot, F., and
29 Horowitz, L. W.: Observational constraints on glyoxal production from isoprene oxidation

1 | and its contribution to organic aerosol over the Southeast United States, ~~in preparation,~~
2 | ~~2015~~[Geophys. Res. Lett., submitted, 2016.](#)

3 | Liu, Y. J., Herdinger-Blatt, I., McKinney, K. A., and Martin, S. T.: Production of methyl
4 | vinyl ketone and methacrolein via the hydroperoxyl pathway of isoprene oxidation, *Atmos.*
5 | *Chem. Phys.*, 13, 5715-5730, doi: 10.5194/acp-13-5715-2013, 2013.

6 | Luecken, D. J., Hutzell, W. T., Strum, M. L., and Pouliot, G. A.: Regional sources of
7 | atmospheric formaldehyde and acetaldehyde, and implications for atmospheric modeling,
8 | *Atmos. Env.*, 47, 477-490, doi: 10.1016/j.atmosenv.2011.10.005, 2012.

9 | Mao, J., Horowitz, L. W., Naik, V., Fan, S., Liu, J., and Fiore, A. M.: Sensitivity of
10 | tropospheric oxidants to biomass burning emissions: implications for radiative forcing,
11 | *Geophys. Res. Lett.*, 40, 1241-1246, doi: 10.1002/grl.50210, 2013.

12 | Mao, J., Ren, X., Brune, W. H., Van Duin, D. M., Cohen, R. C., Park, J. H., Goldstein, A. H.,
13 | Paulot, F., Beaver, M. R., Crouse, J. D., Wennberg, P. O., DiGangi, J. P., Henry, S. B.,
14 | Keutsch, F. N., Park, C., Schade, G. W., Wolfe, G. M., and Thornton, J. A.: Insights into
15 | hydroxyl measurements and atmospheric oxidation in a California forest, *Atmos. Chem.*
16 | *Phys.*, 12, 8009-8020, doi: 10.5194/acp-12-8009-2012, 2012.

17 | Marais, E. A., Jacob, D. J., Kurosu, T. P., Chance, K., Murphy, J. G., Reeves, C., Mills, G.,
18 | Casadio, S., Millet, D. B., Barkley, M. P., Paulot, F., and Mao, J.: Isoprene emissions in
19 | Africa inferred from OMI observations of formaldehyde columns, *Atmos. Chem. Phys.*, 12,
20 | 6219-6235, doi: 10.5194/acp-12-6219-2012, 2012.

21 | Marvin, M., Wolfe, G. M., and Salawitch, R., et al.: Evaluating mechanisms for isoprene
22 | oxidation using a constrained chemical box model and SENEX observations of formaldehyde,
23 | in preparation, 2015.

24 | McNeill, V. F., Woo, J. L., Kim, D. D., Schwier, A. N., Wannell, N. J., Sumner, A. J., and
25 | Barakat, J. M.: Aqueous-Phase Secondary Organic Aerosol and Organosulfate Formation in
26 | Atmospheric Aerosols: A Modeling Study, *Env. Sci. Technol.*, 46, 8075-8081, doi:
27 | 10.1021/es3002986, 2012.

1 Millet, D. B., Jacob, D. J., Boersma, K. F., Fu, T. M., Kurosu, T. P., Chance, K., Heald, C. L.,
2 and Guenther, A.: Spatial distribution of isoprene emissions from North America derived
3 from formaldehyde column measurements by the OMI satellite sensor, *J. Geophys. Res.*
4 *Atmos.*, 113, D02307, doi: 10.1029/2007jd008950, 2008.

5 Millet, D. B., Jacob, D. J., Turquety, S., Hudman, R. C., Wu, S. L., Fried, A., Walega, J.,
6 Heikes, B. G., Blake, D. R., Singh, H. B., Anderson, B. E., and Clarke, A. D.: Formaldehyde
7 distribution over North America: Implications for satellite retrievals of formaldehyde columns
8 and isoprene emission, *J. Geophys. Res. Atmos.*, 111, D24S02, doi: 10.1029/2005jd006853,
9 2006.

10 [Misztal, P. K., Karl, T., Weber, R., Jonsson, H. H., Guenther, A. B., and Goldstein, A. H.:](#)
11 [Airborne flux measurements of biogenic volatile organic compounds over California, *Atmos.*](#)
12 [Chem. Phys., 14, 10631-10647, doi: 10.5194/acpd-14-10631-2014, 2014.](#)

13 Naik, V., Horowitz, L. W., Fiore, A. M., Ginoux, P., Mao, J., Aghedo, A. M., and Levy, H.,
14 II: Impact of preindustrial to present-day changes in short-lived pollutant emissions on
15 atmospheric composition and climate forcing, *J. Geophys. Res. Atmos.*, 118, 8086-8110, doi:
16 10.1002/jgrd.50608, 2013.

17 Palmer, P. I., Abbot, D. S., Fu, T. M., Jacob, D. J., Chance, K., Kurosu, T. P., Guenther, A.,
18 Wiedinmyer, C., Stanton, J. C., Pilling, M. J., Pressley, S. N., Lamb, B., and Sumner, A. L.:
19 Quantifying the seasonal and interannual variability of North American isoprene emissions
20 using satellite observations of the formaldehyde column, *J. Geophys. Res. Atmos.*, 111,
21 D12315, doi: 10.1029/2005jd006689, 2006.

22 Palmer, P. I., Jacob, D. J., Fiore, A. M., Martin, R. V., Chance, K., and Kurosu, T. P.:
23 Mapping isoprene emissions over North America using formaldehyde column observations
24 from space, *J. Geophys. Res. Atmos.*, 108, 4180, doi: 10.1029/2002jd002153, 2003.

25 Paulot, F., Crounse, J. D., Kjaergaard, H. G., Kroll, J. H., Seinfeld, J. H., and Wennberg, P.
26 O.: Isoprene photooxidation: new insights into the production of acids and organic nitrates,
27 *Atmos. Chem. Phys.*, 9, 1479-1501, 2009a.

1 Paulot, F., Crounse, J. D., Kjaergaard, H. G., Kurten, A., St Clair, J. M., Seinfeld, J. H., and
2 Wennberg, P. O.: Unexpected Epoxide Formation in the Gas-Phase Photooxidation of
3 Isoprene, *Science*, 325, 730-733, doi: 10.1126/science.1172910, 2009b.

4 Peeters, J., Muller, J.-F., Stavrou, T., and Nguyen, V. S.: Hydroxyl Radical Recycling in
5 Isoprene Oxidation Driven by Hydrogen Bonding and Hydrogen Tunneling: The Upgraded
6 LIM1 Mechanism, *J. Phys. Chem. A*, 118, 8625-8643, doi: 10.1021/jp5033146, 2014.

7 Peeters, J. and Müller, J. F.: HOx radical regeneration in isoprene oxidation via peroxy radical
8 isomerisations. II: experimental evidence and global impact, *Phys. Chem. Chem. Phys.*, 12,
9 14227-14235, doi: 10.1939/c0cp00811g, 2010.

10 Peeters, J., Nguyen, T. L., and Vereecken, L.: HOx radical regeneration in the oxidation of
11 isoprene, *Phys. Chem. Chem. Phys.*, 11, 5935-5939, doi: 10.1039/b908511d, 2009.

12 Peeters, J., Vandenberg, S., Piessens, E., and Pultau, V.: H-atom abstraction in reactions of
13 cyclic polyalkenes with OH, *Chemosphere*, 38, 1189-1195, 1999.

14 Pollack, I., Lerner, B., and Ryerson, T.: Evaluation of ultraviolet light-emitting diodes for
15 detection of atmospheric NO₂ by photolysis - chemiluminescence, *J. Atmos. Chem.*, 65, 111-
16 125, doi: 10.1007/s10874-011-9184-3, 2010.

17 Rivera-Rios, J. C., Nguyen, T. B., Crounse, J. D., Jud, W., St Clair, J. M., Mikoviny, T.,
18 Gilman, J. B., Lerner, B. M., Kaiser, J. B., de Gouw, J., Wisthaler, A., Hansel, A., Wennberg,
19 P. O., Seinfeld, J. H., and Keutsch, F. N.: Conversion of hydroperoxides to carbonyls in field
20 and laboratory instrumentation: Observational bias in diagnosing pristine versus
21 anthropogenically controlled atmospheric chemistry, *Geophys. Res. Lett.*, 41, 8645-8651, doi:
22 10.1002/2014gl061919, 2014.

23 Roberts, J. M., Marchewka, M., Bertman, S. B., Goldan, P., Kuster, W., de Gouw, J.,
24 Warneke, C., Williams, E., Lerner, B., Murphy, P., Apel, E., and Fehsenfeld, F. C.: Analysis
25 of the isoprene chemistry observed during the New England Air Quality Study (NEAQS)
26 2002 intensive experiment, *J. Geophys. Res.*, 111, D23S12, doi: 10.1029/2006jd007570,
27 2006.

1 Ryerson, T., Huey, L., Knapp, K., Neuman, J., Parrish, D., Sueper, D., and Fehsenfeld, F.:
2 Design and initial characterization of an inlet for gas-phase NO_y measurements from aircraft,
3 *J. Geophys. Res. Atmos.*, 104, 5483-5492, doi: 10.1029/1998JD100087, 1999.

4 Shim, C., Wang, Y., Choi, Y., Palmer, P. I., Abbot, D. S., and Chance, K.: Constraining
5 global isoprene emissions with Global Ozone Monitoring Experiment (GOME) formaldehyde
6 column measurements, *J. Geophys. Res.*, 110, D24301, doi: 10.1029/2004jd005629, 2005.

7 [St. Clair, J. M., Wolfe, G. M., Rivera-Rios, J. C., Crouse, J. D., Praske, E., Kim, M. J.,](#)
8 [Thayer, M. P., Skog, K. M., Keutsch, F. N., Wennberg, P. O., and Hanisco, T. F.:](#)
9 [Investigation of a potential HCHO measurement artifact from ISOPOOH, in preparation,](#)
10 [2016.](#)

11 Stavrou, T., Müller, J.-F., de Smedt, I., Van Roozendaal, M., van der Werf, G. R., Giglio,
12 L., and Guenther, A.: Evaluating the performance of pyrogenic and biogenic emission
13 inventories against one decade of space-based formaldehyde columns, *Atmos. Chem. Phys.*,
14 9, 1037-1060, 2009.

15 Stavrou, T., Müller, J. F., Bauwens, M., De Smedt, I., Van Roozendaal, M., Guenther, A.,
16 Wild, M., and Xia, X.: Isoprene emissions over Asia 1979-2012: impact of climate and land-
17 use changes, *Atmos. Chem. Phys.*, 14, 4587-4605, doi: 10.5194/acp-14-4587-2014, 2014.

18 Stroud, C., Roberts, J., Goldan, P., Kuster, W., Murphy, P., Williams, E., Hereid, D., Parrish,
19 D., Sueper, D., Trainer, M., Fehsenfeld, F., Apel, E., Riemer, D., Wert, B., Henry, B., Fried,
20 A., Martinez-Harder, M., Harder, H., Brune, W., Li, G., Xie, H., and Young, V.: Isoprene and
21 its oxidation products, methacrolein and methylvinyl ketone, at an urban forested site during
22 the 1999 Southern Oxidants Study, *J. Geophys. Res. Atmos.*, 106, 8035-8046, doi:
23 10.1029/2000JD900628, 2001.

24 Trainer, M., Williams, E., Parrish, D., Buhr, M., Allwine, E., Westberg, H., Fehsenfeld, F.,
25 and Liu, S.: Models and observations of the impact of natural hydrocarbons on rural ozone,
26 *Nature*, 329, 705-707, doi: 10.1038/329705a0, 1987.

27 [Valin, L. C., Fiore, A. M., Chance, K., and González Abad, G.: The role of OH production in](#)
28 [interpreting the variability of CH₂O columns in the southeast U.S. *J. Geophys. Res. Atmos.*,](#)
29 [doi: 10.1002/2015JD024012, 2016.](#)

1 Wagner, N. L., Brock, C. A., Angevine, W. M., Beyersdorf, A., Campuzano-Jost, P., Day, D.,
2 de Gouw, J. A., Diskin, G. S., Gordon, T. D., Graus, M. G., Holloway, J. S., Huey, G.,
3 Jimenez, J. L., Lack, D. A., Liao, J., Liu, X., Markovic, M. Z., Middlebrook, A. M.,
4 Mikoviny, T., Peischl, J., Perring, A. E., Richardson, M. S., Ryerson, T. B., Schwarz, J. P.,
5 Warneke, C., Welti, A., Wisthaler, A., Ziemba, L. D., and Murphy, D. M.: In situ vertical
6 profiles of aerosol extinction, mass, and composition over the southeast United States during
7 SENEX and SEAC4RS: observations of a modest aerosol enhancement aloft, *Atmos. Chem.*
8 *Phys.*, 15, 7085-7102, doi: 10.5194/acp-15-7085-2015, 2015.

9 Warneke, C., de Gouw, J. A., Del Negro, L., Brioude, J., McKeen, S., Stark, H., Kuster, W.
10 C., Goldan, P. D., Trainer, M., Fehsenfeld, F. C., Wiedinmyer, C., Guenther, A. B., Hansel,
11 A., Wisthaler, A., Atlas, E., Holloway, J. S., Ryerson, T. B., Peischl, J., Huey, L. G., and
12 Hanks, A. T. C.: Biogenic emission measurement and inventories determination of biogenic
13 emissions in the eastern United States and Texas and comparison with biogenic emission
14 inventories, *J. Geophys. Res. Atmos.*, 115, D00F18, doi: 10.1029/2009jd012445, 2010.

15 Warneke, C., Trainer, M., de Gouw, J. A., Parrish, D. D., Fahey, ~~D. W.~~, Ravishankara, A. R.,
16 Middlebrook, A. M., Brock, C. A., Roberts, J. M., Brown, S. S., Neuman, J. A., Lerner, ~~B.~~
17 ~~M.~~, Lack, D., Law, D., ~~Huebler~~~~Huebler~~, G., Pollack, I., Sjostedt, S., Ryerson, T. B., Gilman, J.
18 B., Liao, J., Holloway, J., Peischl, J., Nowak, J. B., Aikin, K., Min, K. E., Washenfelder, R.
19 A., Graus, ~~M. G.~~, Richardson, M., Markovic, ~~M. Z.~~, Wagner, ~~N. L.~~, Welti, A., Veres, ~~P. R.~~,
20 Edwards, P., Schwarz, J. P., Gordon, T., Dube, W. ~~BP.~~, McKeen, S., Brioude, J., Ahmadov,
21 R., Bougiatioti, A., Lin, J., Nenes, A., Wolfe, G. M., Hanisco, ~~T. F.~~, Lee, B. H., Lopez-
22 Hilfiker, F. D., Thornton, ~~J. A.~~, Keutsch, ~~F. N.~~, Kaiser, J., Mao, J., and Hatch, ~~C. D.~~:
23 Instrumentation and Measurement Strategy for the NOAA SENEX Aircraft Campaign as Part
24 of the Southeast Atmosphere Study 2013, ~~in preparation, 2015~~*Atmos. Meas. Tech. Discuss.*,
25 ~~2016, 1-39, doi: 10.5194/amt-2015-388, 2016.~~

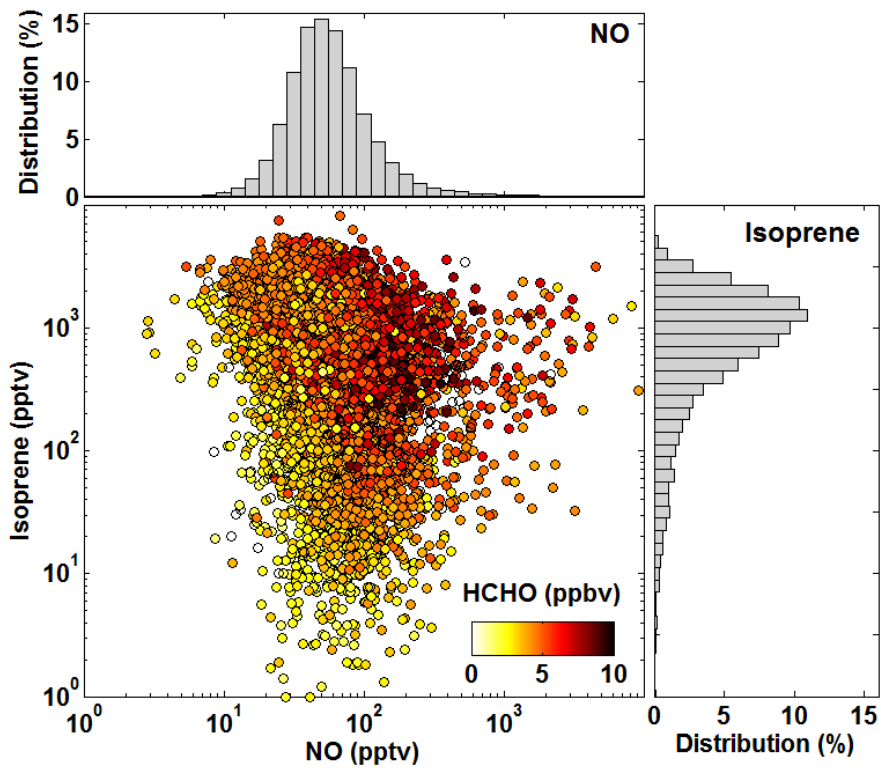
26 Wolfe, G. M., Cantrell, C., Kim, S., Mauldin III, R. L., Karl, T., Harley, P., Turnipseed, A.,
27 Zheng, W., Flocke, F., Apel, E. C., Hornbrook, R. S., Hall, S. R., Ullmann, K., Henrey, S. B.,
28 DiGangi, J. P., Boyle, E. S., Kaser, L., Schnitzhofer, R., Hansel, A., Graus, M., Nakashima,
29 Y., Kajii, Y., Guenther, A., and Keutsch, F. N.: Missing peroxy radical sources within a
30 summertime ponderosa pine forest, *Atmos. Chem. Phys.*, 14, 4715-4732, doi: 10.5194/acp-
31 14-4715-2014, 2014.

1 Wolfe, G. M., Crounse, J. D., Parrish, J. D., St. Clair, J. M., Beaver, M. R., Paulot, F., Yoon,
2 T. P., Wennberg, P. O., and Keutsch, F. N.: Photolysis, OH reactivity and ozone reactivity of
3 a proxy for isoprene-derived hydroperoxyenals (HPALDs), *Phys. Chem. Chem. Phys.*, 14,
4 7276-7286, doi: 10.1039/c2cp40388a, 2012.

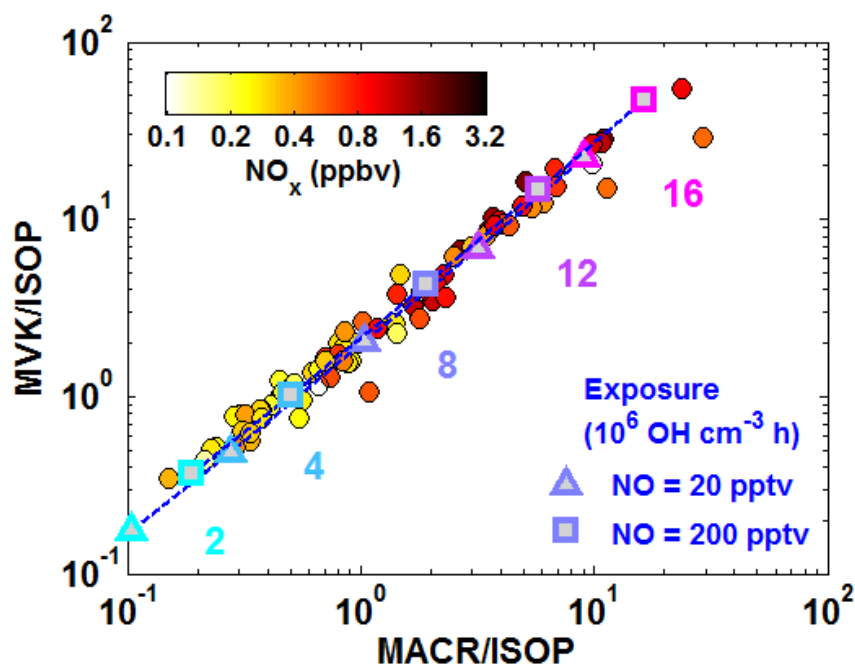
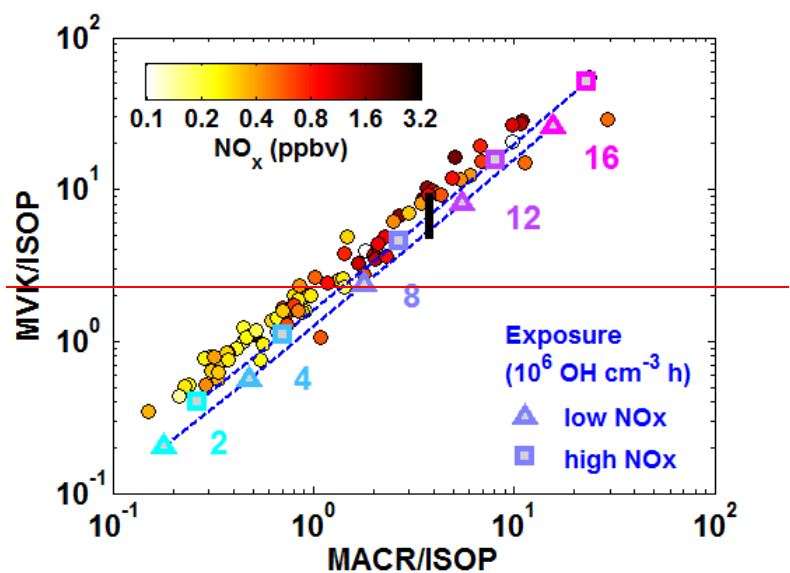
5 [Wolfe, G. M., Hanisco, T. F., Arkinson, H. L., Bui, T. P., Crounse, J. D., Dean-Day, J.,](#)
6 [Goldstein, A., Guenther, A., Hall, S. R., Huey, G., Jacob, D. J., Karl, T., Kim, P. S., Liu, X.,](#)
7 [Marvin, M. R., Mikoviny, T., Misztal, P. K., Nguyen, T. B., Peischl, J., Pollack, I., Ryerson,](#)
8 [T., St Clair, J. M., Teng, A., Travis, K. R., Ullmann, K., Wennberg, P. O., and Wisthaler, A.:](#)
9 [Quantifying sources and sinks of reactive gases in the lower atmosphere using airborne flux](#)
10 [observations, *Geophys. Res. Lett.*, 42, 8231-8240, doi: 10.1002/2015GL065839, 2015.](#)

11 Xu, L., Guo, H., Boyd, C. M., Klein, M., Bougiatioti, A., Cerully, K. M., Hite, J. R.,
12 Isaacman-VanWertz, G., Kreisberg, N. M., Knote, C., Olson, K., Koss, A., Goldstein, A. H.,
13 Hering, S. V., de Gouw, J., Baumann, K., Lee, S.-H., Nenes, A., Weber, R. J., and Ng, N. L.:
14 Effects of anthropogenic emissions on aerosol formation from isoprene and monoterpenes in
15 the southeastern United States, *P. Nat. Acad. Sci. USA*, 112, 37-42, doi:
16 10.1073/pnas.1417609112, 2015.

17



1
 2
 3 **Figure 1.** Co-variation of isoprene, NO and HCHO mixing ratios in the summertime
 4 Southeast U.S. Data are limited to daytime boundary layer observations. Histograms show the
 5 corresponding NO and isoprene distributions.
 6



1

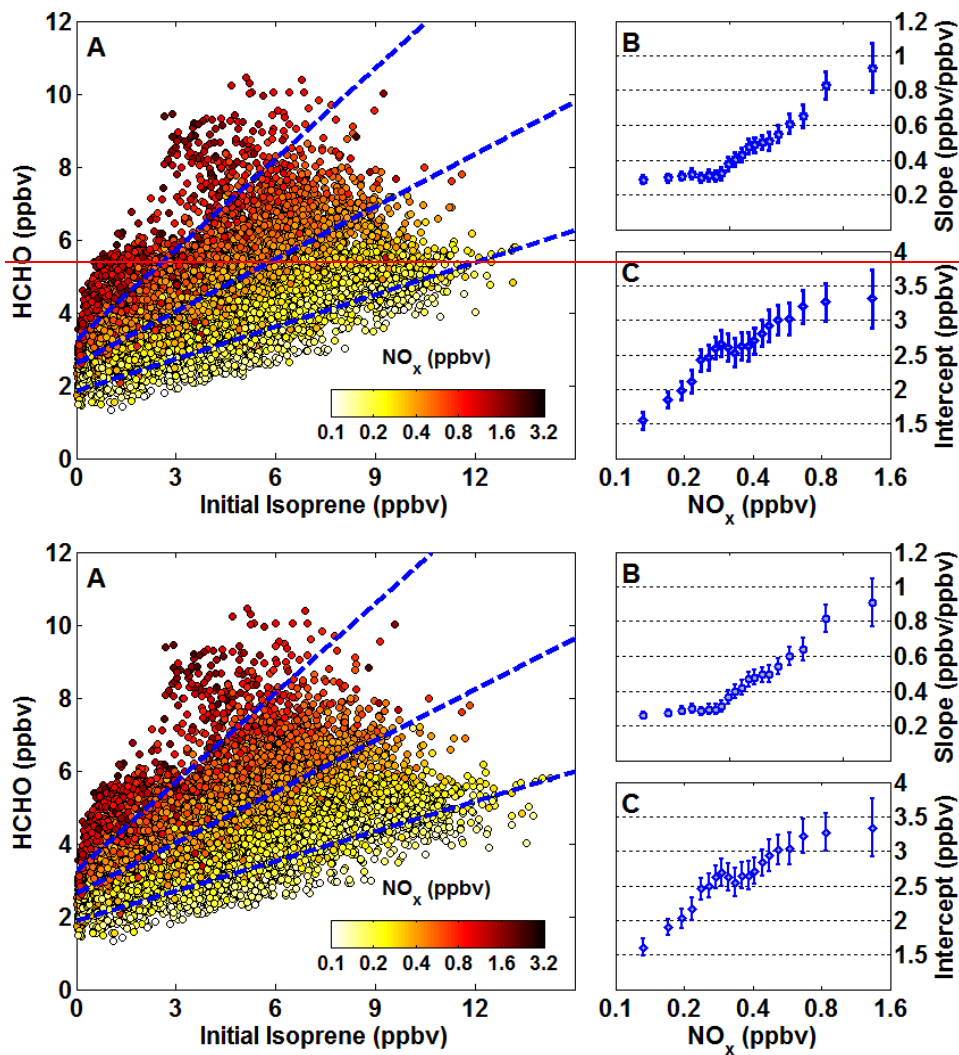
2

3

4 **Figure 2.** A photochemical clock of isoprene oxidation defined by the progression of
 5 daughter/parent ratios. Solid circles show the observed ratios calculated from iWAS

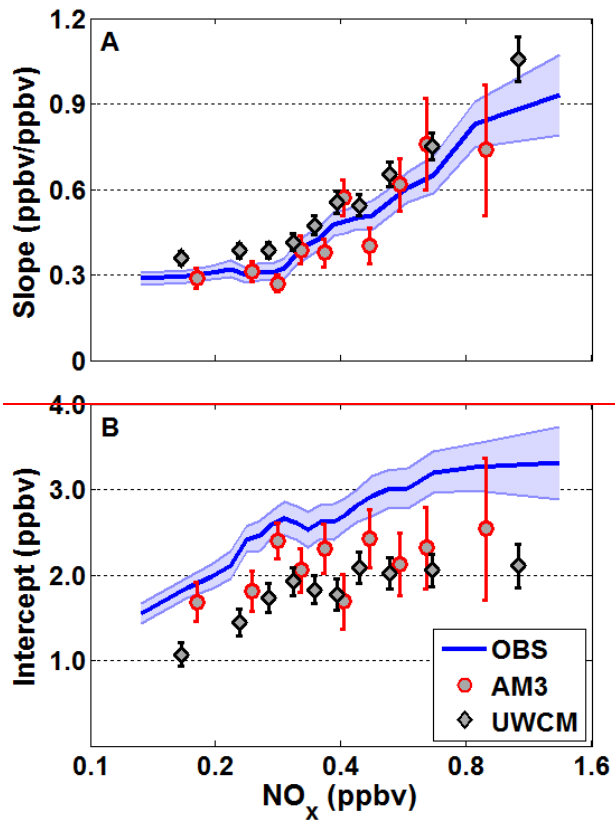
1 observations, colored by NO_x. Blue/purple symbols, dashed lines, and text indicate the
2 theoretical exposures (the product of OH concentration and time) corresponding to any given
3 daughter/parent relationship. Theoretical values are calculated at 298K using MVK and
4 MACR yields for NO values of ~~5020~~ pptv (triangles) and ~~1000200~~ pptv (squares). ~~The thick~~
5 ~~black line denotes the potential systematic error due to an upper limit 51% positive artifact in~~
6 ~~MVK observations (see SI).~~

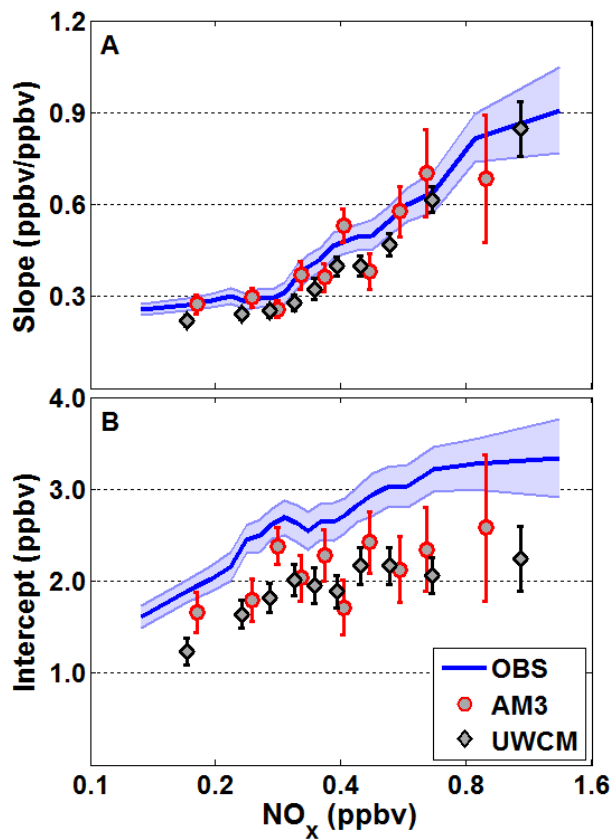
7



1
2
3
4
5
6
7
8
9
10

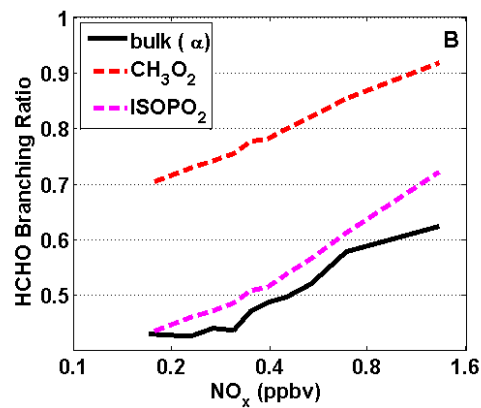
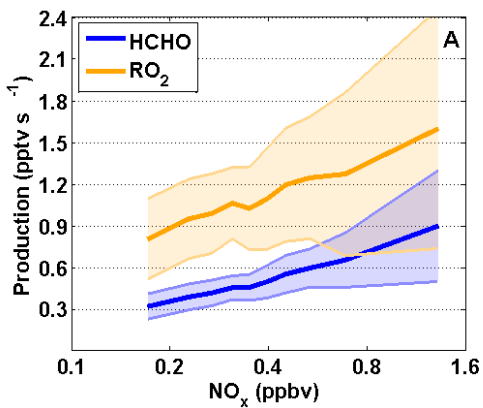
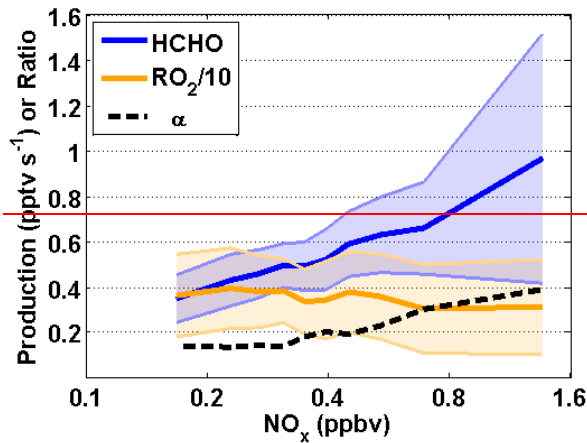
Figure 3. (A) NO_x modulates the relationship between observed HCHO and calculated initial isoprene mixing ratios. Symbols denote all 1-second data. Dashed lines illustrate representative major-axis fits of NO_x-grouped subsets at mean NO_x values of 170, 380 and 810 pptv (see text for details of fitting procedure). The slope (B) and intercept (C) of these fits are the prompt HCHO yield and background HCHO mixing ratio, respectively. Error bars in (B) and (C) are 3σ fitting uncertainties.





1
2
3
4
5
6
7
8

Figure 4. Comparison of observed and model-derived relationships between HCHO and initial isoprene versus NO_x . Slopes (A) and intercepts (B) are calculated as described in the text. The observed values (blue line with shading) are the same as those shown in Figs. 3B-C. Symbols represent fit results for the global AM3 model (red circles) and the 0-D UWCM box model (black diamonds). Error bars denote 3σ fitting uncertainties.



1

2

3

4 **Figure 5.** NO_x dependence of chemical properties related to HCHO production, extracted
 5 from the UWCM simulation of SENEX observations. (A) Production rates for HCHO (blue)
 6 and total RO_2 (orange). (B) Branching ratios for HCHO production weighted over all RO_2
 7 (solid black line) and for several individual RO_2 , including methyl peroxy radical (red) and
 8 total isoprene hydroxyperoxy radicals (magenta). All quantities are averaged over NO_x using
 9 10 bins with equal numbers of points. Solid lines show the mean, and shading is
 10 1σ variability. Note that RO_2 production is scaled down by a factor of 10. The ratio of HCHO
 11 to RO_2 production gives the bulk HCHO branching ratio (dashed line).